LA-8212
(ISPO-77)

Application of Nondestructive Gamma-Ray and Neutron Techniques for the Safeguarding of Irradiated Fuel Materials

PROGRAM FOR
TECHNICAL ASSISTANCE
TO IAEA SAFEGUARDS

USA
IAEA

Department of Energy
Safeguards & Security

University of California

LOS ALAMOS SCIENTIFIC LABORATORY
Post Office Box 1663 Los Alamos, New Mexico 87545

CONTENTS

APPLICATION OF NONDESTRUCTIVE GAMMA-RAY AND NEUTRON TECHNIQUES FOR THE SAFEGUARDING OF IRRADIATED FUEL MATERIALS

by

J. R. Phillips, J. K. Halbig, D. M. Lee, S. E. Beach, T. R. Bement, E. Dermendjiev, C. R. Hatcher, K. Kaieda, and E. G. Medina

ABSTRACT

Nondestructive gamma-ray and neutron techniques were used to characterize the irradiation exposures of irradiated fuel assemblies. Techniques for the rapid measurement of the axial-activity profiles of fuel assemblies have been developed using ion chambers and Be(γ,n) detectors. Detailed measurements using high-resolution gamma-ray spectrometry and passive neutron techniques were correlated with operator-declared values of cooling times and burnup.

EXECUTIVE SUMMARY

Most of the world's inventory of plutonium is stored in the irradiated fuel assemblies of power reactors. The safeguarding of this potential source of weapon material is an essential part of the nuclear nonproliferation policy of the world community. As part of the U.S. technical support program for the International Atomic Energy Agency, we have evaluated the applicability of performing nondestructive measurements on irradiated fuel assemblies. We measured nondestructively passive gamma-ray and neutron signatures of fuel assemblies and correlated these measurements with operator-declared irradiation exposures to establish the usefulness of these techniques to safeguards. These techniques were used in both BWR and PWR fuel assemblies with burnup ranges of 5-18 000 MWd/MTU and 16-38 000 MWd/MTU, respectively.

The gross gamma-ray axial profiles, measured rapidly by using simple ion chambers, correlated well with the ^{137}Cs activity profiles. The gross gamma-ray activity profiles can be used as integrating functions for more detailed measurements performed at a single axial location.

A Be(γ,n) detector was used to measure rapidly the high-energy profiles in which the principal fission product (with energies greater than the lower 1660-keV threshold) is the ^{144}Ce-^{144}Pr 2186-keV gamma ray. The half-life of ^{144}Ce is 284.4 days; therefore this monitor measures the power profiles of the fuel assemblies during the last part of their exposures.

Neutrons originate primarily from the (α,n) reaction and from spontaneous fissioning of the even-numbered plutonium and curium isotopes. Neutrons have greater penetrability than gamma rays; therefore the neutron signature is more representative of the entire fuel assembly. Operator-declared values of burnup correlated with a power function to the measured neutron emission rates. This signature can be influenced significantly by the fuel assembly irradiation history because of the decay characteristics of the ^{242}Cm precursors (^{242}Cm has a half-life of 162.8 days). After the decay of the ^{242}Cm, ^{244}Cm becomes the primary source of neutrons in a fuel assembly and it correlates well with burnup.

We used high-resolution gamma-ray spectrometry to determine the relative burnup values of reactor fuel assemblies. If the irradiation histories are known, operator-declared cooling times can be verified by calculating the expected fission product inventories at discharge. Consistency of cooling times of fuel assemblies irradiated under similar conditions can be verified by plotting the operator-declared values versus the relative activities.

Each of the nondestructive techniques provides some information about an irradiated fuel assembly, but by combining these techniques, the level of confidence of nondestructive measurements is raised to the highest practical level.

I. INTRODUCTION

Nonproliferation is a most critical issue facing the international nuclear community. The International Atomic Energy Agency (IAEA) has been delegated the responsibility of establishing and administering safeguards to detect diversion of special fissionable materials from peaceful to military purposes.[1] The objectives of nonproliferation can be achieved only by the development and application of a safeguards system that is timely and sensitive. At present, from the nonproliferation viewpoint, the most critical area

of the fuel cycle is the post-reactor segment, including reprocessing, conversion to PuO_2, and fuel fabrication.[2] Most of the world's plutonium is in irradiated fuel assemblies that are stored at dispersed reactor facilities. These plutonium stockpiles are potential proliferation hazards.[3]

The number of nuclear power reactors and research reactors coming under IAEA safeguards agreements[4] has increased rapidly within the past few years. In 1971, only 9 power reactors and 66 research reactors were under IAEA safeguards.[5] By December 31, 1977, 100 power reactors and 169 research reactors were under Nonproliferation Treaty (NPT) safeguards, and under non-NPT safeguards for those reactors in non-nuclear weapon states.[6] In 1977, over 30 000 kg of plutonium were contained in irradiated fuel materials in reactor cores and reactor cooling ponds.[6] This quantity is increasing at an accelerating rate as more reactors begin operation. In the United States, for example, the number of spent-fuel assemblies is projected to be 25 000 by 1980 and over 100 000 by 1990.[7]

To provide the required safeguards of irradiated fuel materials in storage facilities, the IAEA relies primarily on containment and surveillance. In addition, nondestructive measurements are required: (1) to establish the initial inventory of a facility, and (2) to verify the inventory of fuel assemblies when the integrity of the containment and surveillance system has failed. Nondestructive techniques can also be used during the routine inspection of a facility as well as at other stages of the fuel cycle, such as at the input to a reprocessing facility.

To assist the IAEA in developing accurate nondestructive techniques, the United States is providing direct technical assistance to the IAEA through the U.S. Initiative Program administered by the International Safeguards Project Office. Under this assistance program, the Los Alamos Scientific Laboratory (LASL) was assigned the task of developing and testing nondestructive passive gamma-ray and passive neutron techniques for characterizing irradiated Light Water Reactor (LWR) fuel assemblies.[8] The principal safeguard concern of irradiated fuel assemblies is the plutonium content, which cannot be measured directly using passive techniques. Plutonium content can be correlated with the total exposure or burnup of the fuel material; therefore, we have investigated the passive gamma-ray and neutron signatures that are correlated to the fuel burnup.

There are many practical problems, as well as measurement problems, associated with the verification of spent-fuel assemblies. An inspection must be completed within a short time because IAEA personnel are limited to the maximum of one-sixth of a man-year for inspection of each reactor facility.[4] Both transportation and installation of measurement instruments are important considerations in the applicability of nondestructive techniques. Also, the type and quality of a fuel assembly's irradiation history data can determine which measurements can be used to estimate the fissile content of fuel assemblies. We have considered the practical problems as well as the measurement problems in our evaluation of nondestructive techniques.

The applicability of nondestructive techniques to the characterization of irradiated fuel assemblies has been reviewed.[9,10] As an integral part of this task, we have reviewed the availability of current technology used in characterizing LWR fuel assemblies.[11] Based upon this review and the recommendations of the IAEA Advisory Group on the Nondestructive Analysis of Irradiated Power Reactor Fuel,[12] we identified and evaluated a variety of nondestructive methods for their applicability in characterizing fuel assemblies. The techniques can be separated into two general categories: gamma-ray methods and neutron methods. The gamma-ray techniques include the use of high-resolution gamma-ray spectrometry (HRGS), gross gamma detectors, and energy-specific detectors. Neutron methods include the use of fission chambers for measuring the neutrons emitted from the assemblies.

TABLE I

CHARACTERISTICS OF FUEL ASSEMBLIES

Type Assembly	Burnup Range	Cooling Time (days)	Fissile Material (% ^{235}U)
MTR	27.4-33.5 at.%	554-1456	93
BWR	4 356-18 804 MWd/MTU	302-1452	2.5-4.5
PWR	16 604-32 185 MWd/MTU	140-837	2.2-2.8
PWR	18 813-38 860 MWd/MTU	120-1200	2.2-3.3
BWR	7 400-11 450 MWd/MTU	627-630	2.56

These techniques were used in the examination of Materials Testing Reactor (MTR), Boiling Water Reactor (BWR), and Pressurized Water Reactor (PWR) fuel assemblies. The characteristics of the specific fuel assemblies are listed in Table I.

This report summarizes the experimental apparatus, results, and conclusions of these examinations and presents recommendations for additional investigations.

II. BACKGROUND

A. Gamma-Ray Techniques

Gamma-ray signatures of irradiated fuel assemblies originate from the fission products of the fuel and the activation products of the cladding and associated structural material. Either the gross gamma activity or the gamma-ray spectra can be measured and the results can be correlated with operator-declared values. From the measured activity of a fission-product isotope A_{ij}, the total number of atoms present in the fuel assembly at the end of the irradiation exposure can be calculated from the following relationship.

$$N_i^o = \frac{A_{ij}\, e^{\lambda_i T_c}}{\lambda_i \varepsilon_j B_j} \quad , \tag{1}$$

where

N_i^o = the number of atoms of the ith isotope at the end of irradiation,
A_{ij} = the measured activity of the ith isotope, jth-energy gamma ray,
λ_i = decay constant of the ith isotope,
ε_j = efficiency correction for jth energy, including source self-absorption, detector efficiency, and solid-angle correction,
B_j = branching ratio for the jth-energy gamma ray, and
T_c = time since discharge (end of irradiation).

The number of atoms of a specific isotope present at the time of measurement is just

$$N_i = \frac{A_{ij}}{\lambda_i \varepsilon_j B_j} \quad . \tag{2}$$

The parameters for λ_i and B_j are physical constants, the A_{ij} value can be measured, and a relative ϵ_j value can be obtained using an intrinsic calibration.[13] The value of T_c must be verified if the irradiation history is not known to allow the determination of relative N_i^o values. For a single isotope, the following relates T_c to N_i

$$T_c = \frac{1}{\lambda_i} \ln \left(\frac{N_i^o}{N_i} \right) . \tag{3}$$

For two isotopes,

$$T_c = \frac{1}{\lambda_2 - \lambda_1} \ln \left(\frac{N_1}{N_2} \right) + \frac{1}{\lambda_2 - \lambda_1} \ln \left(\frac{N_2^o}{N_1^o} \right) . \tag{4}$$

These equations apply to fission products that are not genetically related and do not contain an isotope that is a daughter of a direct fission product. Equations relating these relationships have been previously developed and will only be summarized here.[14,15]

For the case of genetically related isotopes where the second isotope continues to be formed following irradiation (decay of ^{95}Zr to ^{95}Nb),

$$T_c = \frac{1}{\lambda_2 - \lambda_1} \ln \left[\frac{\frac{N_2^o}{N_1^o} + \frac{\lambda_1}{\lambda_1 - \lambda_2}}{\frac{N_2}{N_1} + \frac{\lambda_1}{\lambda_1 - \lambda_2}} \right] . \tag{5}$$

Similarly, for the case where one of the measured isotopes is a daughter of a direct fission product (decay of ^{140}Ba to ^{140}La),

$$T_c = \frac{1}{\lambda_1 - \lambda_3} \ln \left[\frac{\lambda_1}{\lambda_2 - \lambda_1} \cdot \frac{N_1^o}{N_3^o} \cdot \frac{N_3}{N_2} \right] \tag{6}$$

if the assumption $\lambda_2 >> \lambda_1$ is true. The N_2 is the daughter of N_1, and the N_3 is a direct fission product.

Each of the above equations (3-6) requires knowledge of the N_i^o values at the end of the irradiation exposure. These can be calculated if the irradiation history is known.[16] For consistency verification, the values of N_i^o or N_i^o/N_j^o are required to be constant for the set of assemblies.

Burnup is a measure of the number of fissionable[17] atoms consumed during the irradiation. The burnup of an assembly can be expressed as the number of fissions per 100 heavy nuclides initially present or as the integrated energy released from the fissioning of heavy nuclides.[11] The amounts of fission products produced during the irradiation can be used to estimate the burnup of fuel assemblies. The following equation gives the relationship of N_i to various parameters.[18]

$$\frac{\partial N_i(\bar{r},t)}{\partial t} = \sum_k N_k \int_E Y_k^i \sigma_{f_k} \phi dE + \sum_j \gamma_j^i N_j - \lambda_i N_i - N_i \int_E \sigma_c \phi dE , \qquad (7)$$

where N_k = number of k fissioning nuclides,
Y_k^i = fission yield of k nuclide producing N_i,
σ_{f_k} = fission cross section of the k nuclide,
ϕ = neutron flux,
γ_j^i = probability per atom of N_j forming N_i per unit of time,
N_j = number of j nuclides present,
λ_i = decay constant of N_i, and
σ_c = neutron capture cross section.

The first two terms give the production of N_i from the fission process and from the decay of precursor nuclides. The last two terms represent the loss in N_i caused by its radioactive decay and the capture of neutrons. For a single-neutron group, the production of N_i^o during an irradiation period is approximated by

$$N_i^o \propto \bar{\phi}\bar{\Sigma}_f Y_i\left(1 - e^{-\lambda_i t_k}\right)\frac{1}{\lambda_i} , \qquad (8)$$

where

$\bar{\phi}$ = average neutron flux,

$\bar{\Sigma}_f$ = average macroscopic fission cross section of fissioning isotope,

Y_i = fission yield of the ith isotope,

λ_i = decay constant for the ith isotope, and

t_k = length of irradiation time.

Several conditions must be satisfied for this relationship to hold for a specific irradiation exposure: (1) average neutron flux and spectrum remain constant, (2) concentration of fissioning isotope remains constant, (3) average fission cross section remains unchanged, and (4) the average fission yield remains constant. For a ratio of two nuclides,

$$\frac{N_i^o}{N_j^o} \propto \frac{\lambda_j}{\lambda_i} \frac{Y_i}{Y_j} \frac{(1 - e^{-\lambda_i t_k})}{(1 - e^{-\lambda_j t_k})} \quad . \tag{9}$$

For multiple irradiation exposures,

$$\frac{N_i}{N_j} \propto \frac{Y_i \lambda_j \sum_k \frac{\phi_k}{\bar{\phi}} (1 - e^{-\lambda_i t_k}) e^{-\lambda_i \theta_k}}{Y_j \lambda_i \sum_k \frac{\phi_k}{\bar{\phi}} (1 - e^{-\lambda_i t_k}) e^{-\lambda_j \theta_k}} \quad , \tag{10}$$

where

ϕ_k = neutron flux for the kth time interval,

$\bar{\phi}$ = averaged neutron flux in the reactor, and

θ_k = time from the end of kth irradiation period to the time of discharge.

The above relationship is for a ratio of isotopes that are direct fission products. When ratios include an indirect fission product such as ^{134}Cs, which is an activation product of ^{133}Cs, the relationship becomes considerably more complex because of the production dependence upon the energy distribution of the neutron spectrum and the cross-section resonances in the epithermal energy region.

B. Comparison of Operator-Declared Values With Gamma-Ray Results

The measured gamma-ray and neutron signatures of an irradiated fuel assembly are related to the irradiation history, the time since discharge, and the level of burnup. The specific level of verification is, therefore, related to the availability of independent determination of these three factors.[19] If an assembly's irradiation history is known, the relative concentration of specific isotopes and the values of their ratios at a specified cooling time can be calculated by using established modeling techniques.[16] The irradiation history can be verified independently by measuring the relative power of the reactor by using an independent reactor power monitor,[20] and the cooling time can be established by inspection at time of discharge and by surveillance of the storage area. To verify the consistency of the cooling time T_c, the measured and the calculated* values of the ratio at time of discharge are used. Similarly, the burnup value can be calculated from measured isotopic ratios.

If only the irradiation history is known, the N_i^o/N_j^o values can be calculated for inclusion in Eq. (4), (5), or (6) to allow determination of the T_c values. These values can be correlated with the operator-declared values for T_c. Then the irradiation histories and declared T_c values are used to calculate the N_i^o/N_j^o values that are directly related to the burnup values. If only T_c values are known and if the irradiation histories are assumed to be similar for a set of fuel assemblies (that is, if the N_i^o/N_j^o values are constant at the end of the irradiations for a set of fuel assemblies), the internal consistency of the operator-declared T_c values and the measured relative values can be determined.

The relative internal consistency of a set of measured parameters with the operator-declared values is defined as the agreement between a mathematical model and the measured values. The consistency of a set of data is actually determined by checking for the lack of consistency, that is, by seeing if the operator-declared values do not fit the model under investigation. A consistency check depends on the operator-declared values and cannot check for a systematic error. In applying the consistency method to the measured values and the operator-declared values of cooling times, only errors in the relative values of the cooling times can be detected.

*Calculated using Eq. (4), (5), or (6).

The relative burnup values for a set of fuel assemblies can be determined by using established correlations between isotopic ratios and burnup. These correlations may depend upon the specific type of reactor and may require independent calibration to ensure their applicability to a specific set of fuel assemblies.

When there is no independent information available to establish the irradiation histories or the cooling times, the consistency of the operator-declared values of cooling times and burnups can be determined. The consistency of the declared cooling times of a set of fuel assemblies can be checked only if the assemblies have a constant N_i^o/N_j^o or N_i^o value at the end of irradiation. The consistency of the operator-declared burnup values can be checked only if the relative N_i^o/N_j^o values at the end of irradiation can be related to burnup by using the appropriate functional relationship. The nuclides selected to be used in the two consistency measurements must have different production and decay characteristics.

Application of gamma-ray techniques to the measurement of irradiated fuel assemblies has several limitations based upon the physical properties of gamma rays and the specific gamma-emitting isotopes. One important limitation is the problem of self-attenuation within the fuel assembly. For a BWR 8 by 8 assembly, only ~1% of the ^{137}Cs (661.6-keV) gamma rays produced in the central rods escape the fuel assembly.[11] Therefore, measurements using gamma-ray techniques are used primarily for the exterior rods of LWR fuel assemblies. The advantages and disadvantages of specific gamma-emitting isotopes are summarized in Appendix A. Each of the measurable isotopes has limitations in correlating with cooling times or burnup values. The selection of the "best" correlation for either quantity may depend upon the specific ranges of cooling times and burnup values for the fuel assemblies.

C. Neutron Techniques

There are three primary sources of neutrons in an irradiated fuel assembly: spontaneous fissioning of transuranic isotopes, alpha-neutron (α,n) reactions with light materials, and photoneutron reactions. Each of these sources depends upon the irradiation history of the fuel assembly; the first two are related to the buildup of transuranic isotopes (Appendix B) and the third is related to the buildup of fission products. After the fuel assemblies have cooled for several months, only the spontaneous fission and (α,n) reaction

sources are significant. The photoneutron sources are not important because most fission products with high-energy gamma rays (2.23 MeV) have short half-lives (for example, ^{140}Ba-La with $t_{\frac{1}{2}}$ = 12.8 days); thus, this source of neutrons dies away rapidly.

Because it is not generally possible to distinguish the individual isotopic sources of the neutrons emitted from a fuel assembly, only the gross neutron emission rate has been measured and correlated with operator-declared values. One advantage of neutron techniques over the gamma-ray technique is the high penetrability of neutrons. The high penetrability of neutrons reduces the problem of measuring the interior portions of the assembly. Calculations show that neutrons produced in the interior rods of a PWR assembly contribute as much to the measured signal as the neutrons originating in the exterior rods.[21] The neutron response depends upon the cooling time of the fuel assembly, especially, during the first year after discharge (Appendix B).

D. Comparison of Operator-Declared Values With Neutron Results

Neutron measurement of irradiated fuel assemblies can verify the presence of a neutron-emitting source, but it cannot generally differentiate between the isotopes producing the neutrons. It may, however, be possible to measure the relative contribution from spontaneous fissioning and (α,n) reactions.[22] The neutron emission rate of irradiated fuel assemblies depends upon the irradiation histories and the cooling times. The period in which cooling time significantly influences the neutron rate is a function of burnup (Appendix B). When the cooling time is long, the neutron emission rate may be correlated with the declared burnup value by using an empirically determined functional relationship.[21]

III. EXAMINATION OF IRRADIATED HIGHLY ENRICHED FUEL ELEMENTS

Sixteen irradiated fuel assemblies with similar irradiation histories were examined nondestructively to evaluate the correlation between declared burnup values and cooling times with measured isotopic activities or isotopic ratios.[23] Of the two primary objectives of these examinations, the first was to correlate the measurable parameters with operator-declared values of burnup and cooling time, that is, to provide a method of verifying the consistency of these values. The second objective was to establish practical measurement techniques

that could be applied to the subsequent examinations of LWR fuel assemblies. The set of fuel assemblies examined included assemblies with declared burnup values ranging from 27.44 to 33.48 at. % ^{235}U and cooling times from 513 to 1456 days (Table II). Axial scans were obtained on four assemblies to compare results from rapid profile detectors and HRGS to evaluate the applicability of simple detectors measuring burnup profiles. The profiles are then used as integrating functions for determining the burnup of the entire fuel assembly.

A. Experimental Techniques

The fuel assemblies were irradiated in the Omega West Reactor (OWR) at LASL. This reactor is an 8-MWt, heterogeneous, tank-type research reactor that uses aluminum-clad fuel elements of the MTR type. The reactor core consists of a 4 by 9 array of fuel elements, each containing approximately 220 g of ^{235}U (93% enrichment). Each fuel element is constructed of 18 curved fuel plates, 1.52 mm (0.117 in.) apart in heavy aluminum sideplates. Each fuel plate contains a 61-cm-long sheet (24 in.) of uranium-aluminum alloy that is sandwiched and hot rolled between two 0.51-mm-thick sheets (0.020 in.) of pure aluminum.[24]

TABLE II

MTR FUEL ELEMENTS NONDESTRUCTIVELY MEASURED

Fuel Element No.	Burnup (at. %)	Burnup (g)	Discharge Date	Cooling Time (days)	
E356	33.48	73.87	1/17/74	1350	
E357	32.84	71.64	1/17/74	1456	
E359	31.62	69.46	4/8/74	1268	1374
E361	30.11	67.12	6/13/74	1202	
E363	30.99	69.27	6/13/74	1204	
E364	28.89	63.40	10/3/74	1091	
E368	29.15	65.15	2/24/75	947	1053
E370	27.74	61.36	4/21/75	891	998
E371	27.44	61.36	4/21/75	890	
E372	31.52	70.28	9/8/75	750	
E373	32.17	70.54	9/8/75	858	
E375	30.73	68.38	3/1/76	683	
E378	29.29	65.37	3/22/76	554	
E379	29.78	66.22	3/22/76	662	
E383	28.95	63.37	8/16/76	513	

The operator-declared burnup values were calculated from the irradiation history of the reactor and the estimated errors are approximately 5%. A typical 2-week reactor history is presented schematically in Fig. 1. During this period, the reactor was operated 8 hours/day and at power levels ranging from 44% to 100% full power. This irregular operation introduced additional complications into the calculations of the theoretical activity levels of isotopes and isotopic ratios.

The irradiated fuel assemblies were examined using both nondestructive gamma-ray and neutron techniques. The gamma-ray techniques included HRGS to record gamma-ray spectra (500 to 2300 keV) and Be(γ,n) detectors for high-energy gamma profiles. The neutron emission rates were measured using ^{235}U fission chambers.

The experimental HRGS apparatus is illustrated in Fig. 2. The germanium detector was mounted on a movable platform with a fan-shaped collimator. To obtain an axial scan of an irradiated fuel element, the detector-collimator assembly was translated along the principal axis. Complete gamma-ray spectra

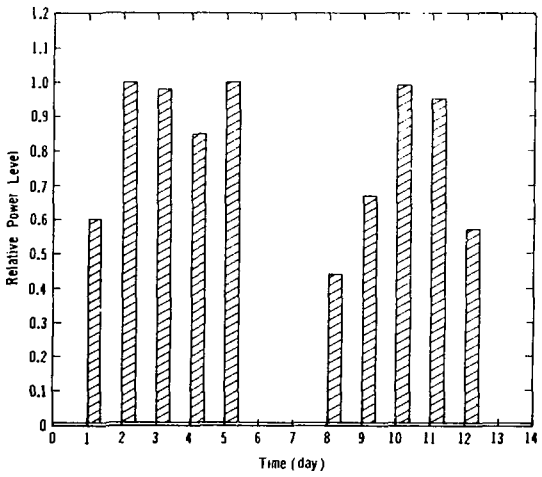

Fig. 1.
Typical two-week irradiation history of an MTR fuel element in the Omega West Reactor.

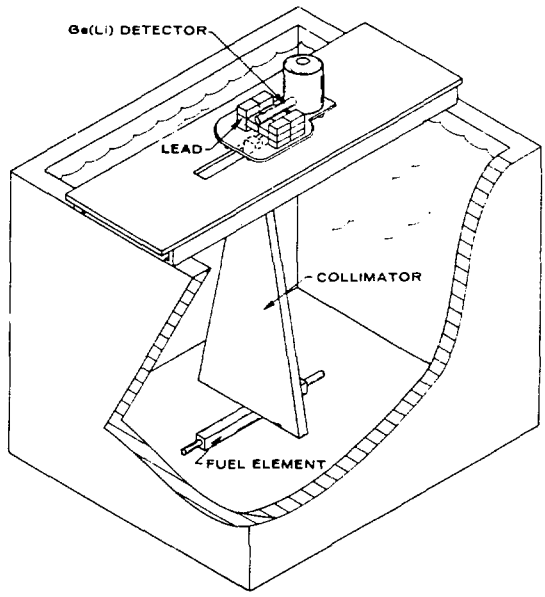

Fig. 2.
Germanium detector and collimator assembly for collection of gamma-ray spectra from MTR fuel elements.

(500-2300 keV) were recorded at specified axial positions and stored on magnetic media for reference. A typical gamma-ray spectra with the major full-energy peaks identified is shown in Fig. 3. The extremely high gamma activity required the insertion of lead (~2.5 cm) as a beam attenuator.

The collimation configuration shown in Fig. 2 was used to measure the axial profiles, with individual gamma-ray spectra collected at specified axial locations. To obtain a gamma-ray spectra that was representative of the entire fuel element, the collimator was rotated 90^{o}. The rotation eliminated the problem of relating a single axial measurement to the entire fuel element (which would require an axial burnup profile). Also, by examining the entire fuel assembly, a better representative value was obtained.

The axial profiles of four fuel elements were measured by using the germanium detector system. The high-energy gross gamma activity profile was obtained by using the Be (γ,n) detector. A high-energy gamma ray (>1660 keV) can undergo an interaction with beryllium, producing a neutron that after being moderated is detected using a ^{235}U fission chamber. A drawing of the Be(γ,n) detector in Fig. 4 shows the relative location of the principal components. The fission chamber is surrounded by a 4-cm-thick polyethylene annulus to moderate the neutrons emitted from the beryllium converter.

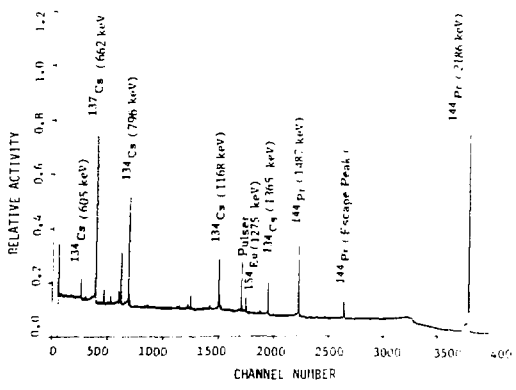

Fig. 3.
Typical gamma-ray spectra showing the principal full-energy peaks.

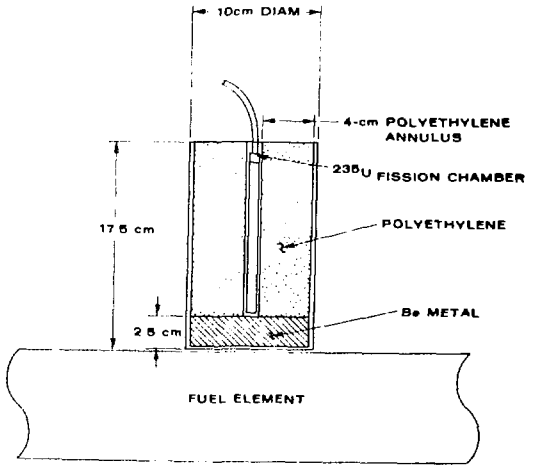

Fig. 4.
Be(γ,n) detector used to measure the high-energy (>1660 keV) gamma-ray profile of MTR fuel elements.

Various thicknesses (0.5, 1.0, 2.0, 3.0, and 4.0 cm) of the polyethylene annulus were evaluated before selecting one 4 cm thick for moderating the neutrons. Thicker discs of beryllium did not improve the detector response significantly. The maximum diameter of the Be(γ,n) detector was restricted by the diameter of the tube. The more compact Be(γ,n) detector designed for the LWR examination exercises is discussed later in this report.

In the typical gamma-ray spectra (Fig. 3), the principal gamma ray interacting with the beryllium and producing neutrons is the 2186-keV gamma ray from the decay of the fission product ^{144}Pr. Because the ^{144}Pr ($t_{1/2}$ = 17.28 minutes) is in secular equilibrium with its parent ^{144}Ce ($t_{1/2}$ = 284.5 days), the axial profile obtained from this detector will represent the more recent irradiation exposure of the fuel element when the irradiation period is significantly longer than the half-life of ^{144}Ce. There is a minor (<2%) contribution from the ^{106}Ru-Rh gamma rays with energies above the 1660-keV threshold. The interference of neutrons emitted from the fuel element was determined to be insignificant (<1%) by removing the beryllium converter and measuring the fission chamber response. Neutrons originate primarily from the (α,n) reaction and spontaneous fissioning of ^{242}Cm, ^{244}Cm, and the even-numbered plutonium isotopes. Because this fuel contained less than 7% ^{238}U, the production of these transuranic isotopes should have been minimal (Appendix B).

The relative neutron profile was measured with a large fission chamber with a 1.6-g loading of ^{235}U. This loading was 40 times larger than that of the small fission chamber (38.6 mg of ^{235}U) in the Be(γ,n) detector.[23]

B. Cooling Times Determined from Gamma-Ray Measurements

The gamma-ray and neutron signatures of irradiated fuel elements are time-dependent variables. Each measurement must be corrected for radioactive decay to allow the data to be correctly interpreted. We have arbitrarily selected the time of discharge as our normalization point. The cooling times for the MTR elements have been determined from the known irradiation histories. The consistency of the operator-declared values has also been checked because the fuel assemblies had been exposed to similar irradiation histories.

1. Calculation of Cooling Times Using Known Irradiation Histories.

a. A simple calculational model has been developed for determining the cooling time of highly enriched fuel assemblies using the detailed irradiation history of each assembly.[25] This technique involves the calculation of the expected activity ratio for two fission products at the end of the irradiation exposure. The ratio is then compared with the experimentally measured ratio at the cooling time T_c. If the detailed irradiation history is not known, a modification of the technique can be used to calculate the approximate cooling time if the length of irradiation is known.

The calculations are based upon a code developed at Battelle Pacific Northwest Laboratory for calculating the fission product activity ratios in irradiated fuel.[26] A small program (COLDET) incorporates the fissioning of ^{235}U, ^{238}U, and ^{239}Pu and the absorption of the neutron by the selected fission products.[25] The neutron flux is assumed to be a constant during each short irradiation period with one set of average thermal cross sections (see Eqs. 8-10).

The calculated cooling times for the two sets of assemblies using the operator-declared irradiation histories are presented in Table III. The relative intrinsic efficiency was determined using the ^{134}Cs and ^{144}Pr gamma rays.[13] The relative efficiency curve was then used to correct the peak areas of the gamma rays listed in Table III. The $^{144}Pr/^{137}Cs$ activity ratio gives the best correlation with the declared cooling times. This confirms the results obtained by other investigators on similar fuel materials.[26,27] For cooling times of <300 days the $^{95}Zr/^{137}Cs$ activity ratio can be used with good precision. The relatively short half-life of ^{95}Zr (63.98 days) limits its applicability to short cooling times.

b. The modified technique in which only the irradiation exposure period is required was similarly used to calculate the cooling times of the fuel assemblies. In this simplified approximation, the reactor is considered to be operating at constant power from the time the fuel is loaded until it is discharged. The cooling-time relation is obtained by inserting Eq. (9) into Eq. (4)

$$T_c = \frac{1}{\lambda_2 - \lambda_1} \ln\left(\frac{N_1}{N_2}\right) + \frac{1}{\lambda_2 - \lambda_1} \ln \frac{\lambda_1 Y_2 (1 - e^{-\lambda_2 t_k})}{\lambda_2 Y_1 (1 - e^{-\lambda_1 t_k})} , \qquad (11)$$

TABLE III

COMPARISON OF DECLARED AND CALCULATED COOLING TIMES USING DETAILED IRRADIATION HISTORIES

Element	Operator-Declared Cooling Time (days)	Calculated Cooling Time[a] Based on Activity Ratio: $^{95}Zr/^{137}Cs$ days	% diff	$^{144}Pr/^{137}Cs$ days	% diff	$^{106}Rh/^{137}Cs$ days	% diff
(Set A)							
E356	1350	902	-33.2	1368	1.3	1314	-2.7
E359	1268	888	-30.0	1296	2.2	1481	16.8
E361	1202	898	-25.3	1149	-4.4	1232	2.5
E363	1204	879	-27.0	1225	1.7	1208	0.3
E364	1091	936	-14.2	1133	3.8	1513	38.7
E368	947	1075	13.5	940	-0.7	941	-0.6
E370	891	902	1.2	849	-4.7	1025	15.0
E371	890	854	-4.0	865	-2.8	1407	58.1
E372	750	790	5.3	758	1.1	797	6.3
E378	554	565	2.0	526	-5.1	666	20.2
Average difference			15.6%		2.8%		16.1%
(Set B)							
E357	1456	950	-34.8	1506	3.4	1479	1.6
E359	1374	976	-29.0	1397	1.7	1351	-1.7
E368	1053	1871	77.7	1057	0.4	1014	-3.7
E370	998	904	-9.4	1021	2.3	1024	2.6
E373	858	834	-2.8	918	7.0	915	6.6
E375	683	687	0.6	728	6.6	785	14.9
E379	662	678	2.4	689	4.1	629	-5.0
Average difference			22.4%		3.6%		7.2%

[a]Gamma-ray lines used: $^{95}Zr/^{137}Cs$ (756 keV/662 keV), $^{144}Pr/^{137}Cs$ (696 keV/662 keV), and $^{106}Rh/^{137}Cs$ (622 keV/662 keV).

where t_k is the irradiation period (Eq. 8). The results for $^{144}Pr/^{137}Cs$ activity ratios in the two sets of data using this approximation have been summarized in Table IV. Precisions for this set of fuel assemblies are comparable to the values obtained using the more detailed irradiation histories because of similarities of irradiation histories.

A detailed analysis of the errors in the cooling time determination using the constant power approximation has been recently completed.[28] The effect of variations in the downtime between cycles, power variations from one cycle to the next, and the variations in the irradiation period were evaluated for

TABLE IV

COOLING TIMES BASED ON APPROXIMATE CALCULATIONAL METHOD AND $^{144}Pr/^{137}Cs$ ACTIVITY RATIO

Element	Irradiated Time (days)	Declared Cooling Time (days)	Calculated Cooling time (days)	Percent Difference
(Set A)				
356	501	1350	1350	0.0
359	541	1268	1306	3.0
361	587	1202	1164	-3.2
363	553	1204	1244	3.3
364	636	1091	1159	6.2
368	751	947	970	2.4
370	764	891	870	-2.4
371	764	890	886	-0.4
372	903	750	769	2.5
378	995	554	500	-9.7
		Average difference		3.3%
(Set B)				
357	501	1456	1495	2.7
359	541	1374	1408	2.5
368	751	1053	1088	3.3
370	764	998	1041	4.3
373	903	858	924	7.7
375	1023	683	727	6.4
379	995	652	652	-1.5
		Average difference		4.1%

the $^{95}Zr/^{137}Cs$ and $^{144}Pr/^{137}Cs$ ratios. The most significant errors were caused by power variations from one cycle to the next, unless the irradiation period was very short. For irradiation periods of more than 100 days, errors caused by power variations are greater for the $^{144}Pr/^{137}Cs$ ratio than for the $^{95}Zr/^{137}Cs$ ratio.[28]

2. Consistency of Declared Cooling Times. The internal consistency of the declared cooling times was evaluated using the relationships for single isotopes and isotopic ratios discussed in Sec. II, Eqs. (3) and (4). In this technique, the values for N_i^o and N_i^o/N_j^o must be constant for the set of fuel assemblies, with the relative T_c values restricted to the line defined by the slope $1/\lambda_i$ or $1/(\lambda_j-\lambda_i)$ for single isotopes and isotopic ratios, respectively. Any T_c value not on this line would be inconsistent with the set, or the assumption of constant N_i^o or N_i^o/N_j^o is not valid.

For each of the MTR exercises, we have correlated selected variables and ratios with the declared cooling times.[23] We have not performed any corrections for variations in burnup values or in the power histories for the elements because the range of burnup values is relatively narrow and the irradiation histories were all very similar. The results from this analysis are shown in Table V; the declared values are compared to the values from the equations, with the slopes being restricted to $1/\lambda$ and $1/(\lambda_2 - \lambda_1)$ for single isotopes and ratios, respectively (Eqs. 4 and 5). The line does not fit all the data because of the restriction placed upon the slopes by the model. This technique provides a rapid method for verifying the consistency of the operator-declared values when the irradiation exposures are similar. The cooling-time values obtained from the regression equation may be shifted by an additive value; however, the relative differences between fuel elements with different cooling times are correct.

The relative activities of ^{144}Pr correlated well with the operator-declared values as is shown in Fig. 5 for the Table V, B set of elements. Similarly, the results for $^{144}Pr/^{137}Cs$ are presented in Fig. 6. Application of this ratio and other ratios has been addressed by other authors.[27,29,30] In general, the ^{106}Rh isotope should be used cautiously: its concentration can be influenced significantly by the original enrichment of the fuel because the fission yield of its precursor, ^{106}Ru differs by a factor of 11 for ^{235}U and ^{239}Pu fissions (Appendix A).

TABLE V

COMPARISON OF DECLARED COOLING TIMES WITH COOLNG TIMES DETERMINED FROM THE REGRESSION EQUATION[a]

Element	Declared Cooling Time (days)	Cooling Times Determined from the Equations[b] (days)				
		^{144}Pr	$^{144}Pr/^{137}Cs$	$^{134}Cs/^{154}Eu$	$^{106}Rh/^{137}Cs$	$^{106}Rh/^{144}Pr$
(Set A)						
E356	1350	1229	1324	1414	1304	1370
E359	1268	1204	1286	1276	1193	1497
E361	1202	1171	1221	1175	1261	1130
E363	1209	1177	1232	1050	1270	1146
E364	1091	1115	1124	1114	1163	1036
E368	947	1017	988	784	961	1049
E370	891	946	893	993	900	877
E371	890	934	891	907	921	822
E372	750	781	715	950	718	709
E378	554	593	491	503	474	529
Average difference[c]		5.1%	3.1%	7.8%	5.1%	5.6%
(Set B)						
E357	1456	1328	1347	1443	1441	1514
E359	1374	1302	1308	1349	1414	1382
E368	1053	1103	1087	1136	1097	1090
E370	998	1022	1002	937	1011	960
E373	858	869	901	813	917	742
E375	683	761	760	688	664	718
E379	662	703	701	723	545	682
Average difference[c]		5.7%	5.4%	4.5%	5.3%	4.8%

[a] For normal applications, the isotopic ratios are preferable to the single isotopes because the ratios are less sensitive to geometric and efficiency factors and data from different investigations may be correlated.

[b] Because this is a consistency measurement, only relative cooling time values can be determined.

[c] Values are the average differences of specific ratios from the calculated regression line.

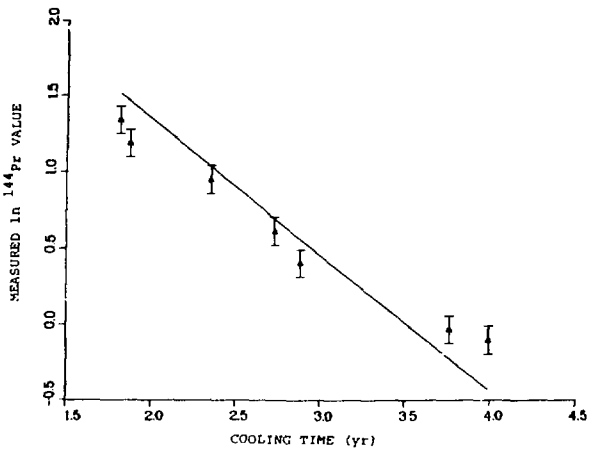

Fig. 5.
Measured ^{144}Pr activity vs operator-declared values of cooling time with a slope of $1/\lambda$.

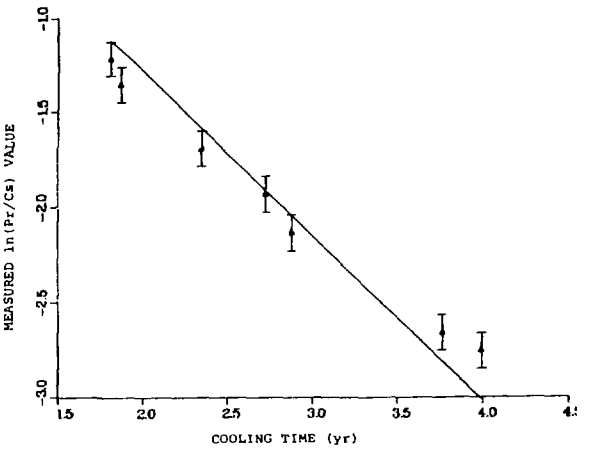

Fig. 6.
Measured ^{144}Pr/^{137}Cs isotopic ratio vs operator-declared values of cooling time with a slope of $1/(\lambda_2-\lambda_1)$.

C. Axial Profile Measurements.

The axial profiles of four elements were measured using the germanium and Be(γ,n) detectors. The axial isotopic distribution of ^{137}Cs was determined from the germanium data and was compared with the Be(γ,n) results obtained using two thicknesses of beryllium (Fig. 7). Comparisons of the ^{137}Cs and Be(γ,n) profiles showed good agreement.

The axial neutron profile was measured using a large fission chamber with a 1.6-g ^{235}U loading.[23] The neutron count rates (2 counts/s) were very low because the 93% ^{235}U initial enrichment of the fuel resulted in the formation of a very small amount of the even-numbered transuranics.

D. Determination of Burnup Values

The measured gamma-ray activities were corrected for decay that occurred since discharge by using the operator-declared cooling times. All burnup calculations were based upon the total grams of fissioned ^{235}U. The initial ^{235}U loadings ranged from 218 to 224 g, and the operator-declared amounts of fissioning ^{235}U ranged from 61 to 74 g.

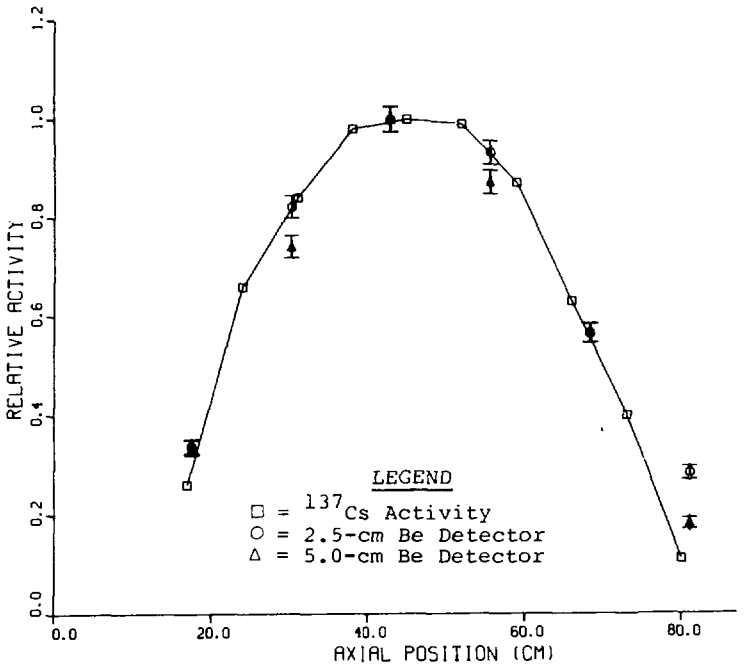

Fig. 7.
Axial profiles of two Be(γ,n) detector configurations and the ^{137}Cs activity.

Selected isotopic variables and ratio of variables have been correlated with the operator-declared burnup values using a linear model.[22] A summary of the results is included in Table VI. For the single isotopes, ^{137}Cs had the best correlation with declared burnup. Isotopic ratios are influenced less by geometrical factors than the single isotopes. Correlations using $^{134}Cs/^{137}Cs$ and $^{154}Eu/^{137}Cs$ had average differences of 2.5-4.0% for both sets.

Each variable can contain some unique information about the parameters in Eq. 7; therefore, the use of a combination of two or more variables may improve the correlation. For these sets of data, the use of two variables improved the correlations, whereas the use of more than two variables did not improve them significantly. Included in Table VI are the linear combinations of ^{137}Cs and $^{134}Cs/^{137}Cs$ for Set A and ^{137}Cs and $^{154}Eu/^{137}Cs$ for Set B. As Table VI shows, the fit of the linear regression line was improved slightly by using two variables. Some of the improvement may have been due to improved counting statistics.

TABLE VI

COMPARISON OF OPERATOR-DECLARED AND RELATIVE BURNUP VALUES BASED UPON A LINEAR CORRELATION[a]

Element	Operator-Declared Burnup (g)	Relative Burnup Calculated from the Regression Equation (g)				
		^{137}Cs	$^{134}Cs/^{137}Cs$	$^{154}Eu/^{137}Cs$	^{137}Cs and $^{134}Cs/^{137}Cs$	^{137}Cs and $^{154}Eu/^{137}Cs$
(Set A)						
E356	73.87	70.84	73.54	69.80	73.21	71.31
E359	69.46	70.03	70.26	68.18	70.65	69.92
E361	67.12	66.98	65.36	65.28	66.23	66.43
E363	69.27	67.28	68.57	64.64	65.95	66.48
E364	63.40	63.85	64.18	65.66	64.01	63.87
E368	65.15	62.76	66.69	63.62	62.14	62.27
E370	61.36	62.68	60.84	65.39	63.50	62.79
E371	61.36	64.33	67.41	67.45	64.28	64.88
E372	70.28	67.54	65.96	70.60	69.06	68.76
E378	65.37	70.37	66.81	65.99	67.36	69.65
Average difference		3.1%	2.8%	4.0%	2.7%	3.1%
(Set B)						
E357	71.64	71.56	70.86	71.56	72.19	71.95
E359	69.46	69.68	69.67	69.20	70.25	69.66
E368	65.15	63.79	63.24	64.27	63.88	63.65
E370	61.36	64.58	66.20	62.86	64.87	63.39
E373	70.54	71.45	69.79	69.21	68.13	70.72
E375	68.38	66.98	66.34	66.40	66.52	66.63
E379	66.22	65.52	66.49	69.25	66.91	67.21
Average difference		1.7%	2.5%	2.6%	2.4%	1.5%

[a]For normal applications, the isotopic ratios are preferable to the single isotopes because the ratios are less sensitive to geometric and efficiency factors and data from different investigations can be correlated.

We are assuming in the above discussion that the correlation between the measured parameters $^{134}Cs/^{137}Cs$ and $^{154}Eu/^{137}Cs$ and the operator-declared burnup values are linear. That is, that

$$\text{Burnup} = A + B \cdot R_i, \tag{12}$$

where A and B are coefficients of the regression equation and R_i is the measured ratio. If the ^{137}Cs activity is directly related to burnup, ^{134}Cs and ^{154}Eu must be proportional to $(^{137}Cs)^2$ for Eq. (12) to be valid. By measuring the axial profiles of four fuel elements, we determined the power relationships of ^{134}Cs and ^{154}Eu activities with the ^{137}Cs activity to be approximately 1.8 for for both isotopes (ranging from 1.6 to 2.0) over this narrow range of burnup values.

Table VII shows the ratio data corrected for the nonlinearity in the relationships of the variables to the declared burnup.

$$\text{Burnup} \propto (\text{Ratio})^{\beta} \tag{13}$$

where β is not equal to 1.0. There appears to be only a slight improvement in the percentage differences. Therefore, adjusting the data over this narrow range of burnup values for the nonlinearity did not significantly improve the quality of the fit.

IV. EXAMINATION OF IRRADIATED BWR FUEL ASSEMBLIES

Ten irradiated BWR fuel assemblies were examined nondestructively to evaluate the correlation between gamma-ray and neutron signatures with operator-declared values for burnup. Table VIII lists the specific BWR fuel assemblies examined in this exercise. Declared burnup values range from an average assembly burnup of 4356 MWd/MTU to 18 804 MWd/MTU with cooling times from 302 to 1452 days.

The individual fuel assemblies were composed of a 9 by 9 array of UO_2 fuel rods with three levels of enrichment in each assembly (2.5%, 3.3%, and 4.5%). These fuel assemblies were shorter than typical BWR assemblies in 1000-MWe facilities. Their active lengths were only 178 cm (70 in.) compared to the nominal 366-cm length (144 in.) of fuel assemblies in 1000-MWe BWR facilities. Physical characteristics of the fuel assemblies are listed in Table IX. The fuel assemblies had been irradiated in the Big Rock Point Nuclear Plant,* which was operated at a maximum rating of 240 MWt or 75 MWe during the irradiation exposures.

*Operated by Consumers Power Company.

TABLE VII

COMPARISON OF DECLARED AND CALCULATED BURNUP VALUES
BASED UPON A NONLINEAR CORRELATION

Element	Declared Burnup (g)	Calculated Burnup (g) $^{134}Cs/^{137}Cs$	Calculated Burnup (g) $^{154}Eu/^{137}Cs$
(Set A)			
E356	73.87	75.97	74.29
E359	69.46	67.59	68.36
E361	67.12	65.71	64.88
E363	69.27	67.21	67.27
E364	63.46	64.38	64.02
E368	65.15	64.87	64.20
E370	61.36	63.94	63.89
E371	61.36	64.05	63.89
E372	70.28	68.04	72.06
E378	65.37	64.95	64.26
Average difference		2.5%	2.3%
(Set B)			
E357	71.64	73.29	72.92
E359	69.46	69.09	67.06
E368	65.15	65.27	65.99
E370	61.36	64.44	65.92
E373	70.54	68.59	68.03
E375	68.38	67.06	66.42
E379	66.72	65.65	66.06
Average difference		2.0%	3.0%

A. Experimental Techniques

The irradiated fuel assemblies were measured nondestructively using both gamma-ray and neutron techniques. Gamma-ray techniques included the use of intrinsic germanium detectors, ion chambers, and a Be(γ,n) detector. The neutron activity was measured by using small ^{235}U fission chambers.

Figure 8 shows the examination apparatus. The detection system was located next to the wall opposite the fuel storage racks. Fuel assemblies were moved to the fuel assembly elevator that provided the mechanism for axial scanning.

TABLE VIII

BWR FUEL ASSEMBLIES EXAMINED NONDESTRUCTIVELY

Fuel Assembly Identification	Delcared Burnup Value (MWd/MTU)	Discharge Date	Declared Cooling Time (days)
BWR-1	4 356	1-76	842
BWR-2	8 883	1-74	1452
BWR-3	13 332	1-76	843
BWR-4	14 652	1-76	842
BWR-5	15 264	1-76	843
BWR-6	16 233	7-77	305
BWR-7	16 658	1-76	842
BWR-8	17 122	1-76	844
BWR-9	17 814	1-76	842
BWR-10	18 804	7-77	302

TABLE IX

PHYSICAL CHARACTERISTICS OF BWR FUEL ASSEMBLIES

Fuel geometry	9 by 9 array
Fuel rods per bundle (standard)	70
Fuel rods per bundle (special)[a]	11
Fuel cladding material	Zircaloy-2
Wall thickness	0.10 cm (0.040 in.)
Diameter of fuel pellets	1.429 cm (0.5625 in.)
Fuel density	94% theoretical
Active fuel length	178 cm (70 in.)
Fill Gas	Helium
Enrichment - ^{235}U	2.5-4.5%

[a]Experimental rods; maximum of 11 in any assembly.

The vertical tube and collimator tube were attached to the side of the storage pool to ensure constant scanning geometry. A Be(γ,n) detector was placed in the vertical tube to obtain profile measurements. This detector was replaced with a fission chamber for the neutron measurements. The ion chamber was suspended in a separate tube on the opposite side of the fuel assemblies. During the measurements we were unable to verify the relative positions of the various detectors with respect to the germanium collimator.

For the axial germanium scans, the fuel assembly was placed in the elevator so the 5-cm-wide collimator was viewing one side of the assembly. Complete gamma-ray spectra (500-2300 keV) were recorded at specified axial positions (usually 33-cm intervals). The principal isotopic gamma rays identified in the spectra were identical to those shown in Fig. 3. The examination time at each axial position ranged from 300 to 1000 s.

Ion chambers are simple detectors that can rapidly measure the axial gamma profiles of irradiated fuel assemblies. These profiles can be used as integrating functions for the entire assembly. The ion chamber used in this examination is shown in Fig. 9.[31] The active area was 3.8 cm by 6.25 cm with a plate spacing of 1.25 cm. The anode wires were 20-μm gold-plated tungsten wire with wire-to-wire spacing of 1.25 cm. The voltage characteristics of the chamber showed that the plateau corresponding to the ionization region (gas gain = unity) was relatively constant from -100 to -1000 V. In this exercise, the ion chamber was operated in the ionization region at -300 V. The readout of the chamber was relatively simple, consisting of a current-to-voltage amplifier and a digital voltmeter. Various fill gases were tested (air, helium, xenon) with the air-filled chamber selected as the best choice.

The Be(γ,n) detector is shown in Fig. 10 and was designed to allow its insertion into the 5-cm-i.d. vertical tube. The neutrons produced in the beryllium annulus are thermalized in the polyethylene and then counted using the ^{235}U fission chamber. Because the threshold for photoneutron production in beryllium is 1660 keV, the only significant gamma ray contributing to this reaction is the 2186-keV gamma ray of ^{144}Pr. The ^{144}Pr isotope with a very short half-life of 17.3 min is in secular equilibrium with its parent ^{144}Ce (284.5 days). Therefore, the Be(γ,n) detector measures the relative activity of ^{144}Ce. There is less than 2% contribution from ^{106}Rh gamma rays with energies above 2000 keV, but this is minor when compared to the ^{144}Pr contribution.

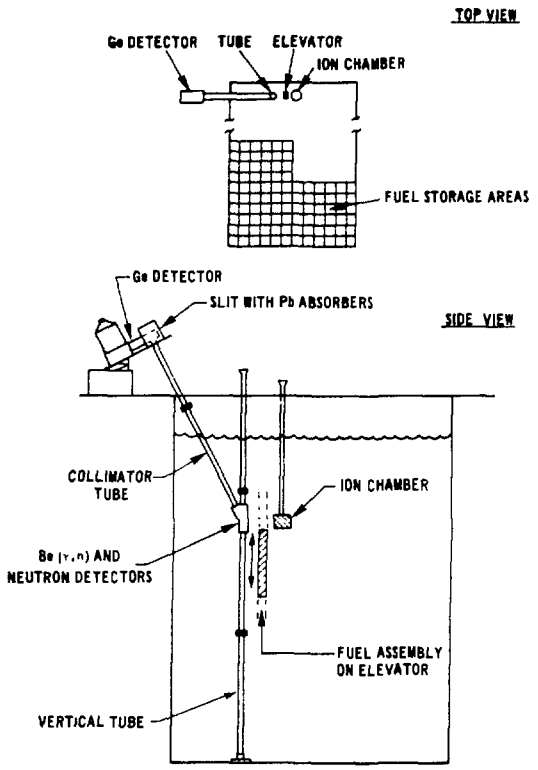

Fig. 8.
Experimental apparatus used for the examination of the BWR fuel assemblies.

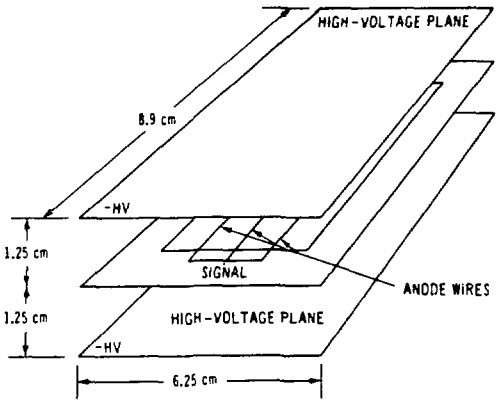

Fig. 9.
Ion chamber used in BWR examinations.

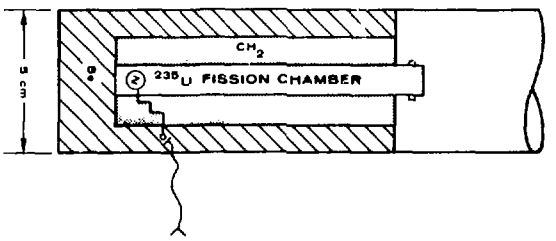

Fig. 10.
Schematic of Be(γ,n) detector showing the beryllium and polyethylene sleeves surrounding the fission chamber.

The ^{235}U fission chambers used to measure the relative neutron emission rates contained 58 mg of fissile material. The physical limitations of the scanning mechanism permitted only about 27 cm between the fuel assembly face and the neutron detector. This source-to-detector distance remained constant during the neutron measurements because a change would have altered the measured rate.*

*The thermal neutron flux decreased an order of magnitude when the source-to-detector distance was increased 10 cm (Ref. 21).

Measurements using all four types of detectors were made at selected axial positions to obtain axial profiles. The measurements recorded at the midplane of the assemblies were used for correlations between the various assemblies.

B. Axial Profile Measurements of BWR Fuel Assemblies

Axial profile measurements can be used to define the physical dimensions of the fuel assemblies as well as to provide an integrating function of the fuel assemblies. Because the burnup varies along the length of the fuel assembly, it is necessary to integrate the entire length to compare results with the operator-declared values for the entire fuel assembly. A rapid measurement of the activity profile coupled with a detailed measurement at one axial position can be used to estimate the relative burnup value of the assembly. In this section, we will discuss the results from four detectors: germanium, Be(γ,n), ion, and neutron. None of these can measure burnup directly, but they measure indirect signatures that can be related to relative burnup values.

All the axial gamma-ray profiles of the BWR fuel assemblies had maxima near the mid-planes of the assemblies. The shape of the activity profiles would not necessarily be symmetrical because (1) the control rods are inserted adjacent to the fuel assemblies, and (2) there are changes in the void fraction in the boiling region of the reactor.

As was discussed in Sec. IV.A, the Be(γ,n) detector is sensitive to gamma-ray energies above 1660 keV, and ^{144}Pr is the only fission product isotope with significant activity above this threshold. Therefore, we must establish that the ^{144}Pr isotopic profile is representative of the axial burnup profile. We have assumed that the ^{137}Cs axial profile (determined from the germanium system) is the best available burnup monitor.[9-11] In Fig. 11, the relative axial profiles are plotted for the ^{137}Cs and ^{144}Pr isotopes and for the gross gamma for the BWR-10 assembly. The ^{137}Cs and ^{144}Pr profiles for all the BWR assemblies were within the measurement uncertainties for all the axial scans. Because ^{144}Ce-^{144}Pr does not migrate, there was no detectable gross axial migration of the ^{137}Cs isotope[11,16] within our 30-cm measurement precision.

The germanium-detector-measured gross gamma profiles of the fuel assemblies were displaced toward the bottom ends of the assemblies when compared to the ^{137}Cs profiles (Fig. 11). The gross gamma data were obtained by setting a lower (approximately 200-keV) level threshold on the germanium system and

summing all the counts above this threshold. We investigated the possibility that this observed shift could be due in part to specific isotopes having a different axial profile from ^{137}Cs. In BWR-6 and 10, the two assemblies with short cooling times, the short-lived isotopes ^{95}Nb and ^{95}Zr contributed approximately 30% of the total observed activity and their profiles were displaced from the ^{137}Cs profiles toward the bottom. Because these isotopes reflect the more recent power history, these differences could be due to power-level differences at the end of the reactor cycle, that is, due to the possible removal of control rods. However, these differences in the ^{95}Zr and ^{95}Nb profiles are not great enough to account for the total observed shift in the gross gamma profile. The fact that all profiles (even those with a long cooling time of more than 800 days when the ^{95}Zr and ^{95}Nb isotopes are no longer significant) were shifted by approximately the same amount suggests that the observed shift may be due to some other mechanism. A possible explanation may be related to the scanning geometry. As the fuel assembly is raised past the end of the collimator, the major portion of the activity of the assembly moves closer to the detector and collimator as a whole, so there is a greater possibility for Compton-scattered gamma rays to scatter into the detector. This could explain the increase in the relative activity observed for the lower portion of the fuel assembly. Thus, gross gamma profiles obtained by using similar collimation geometries may not provide realistic profiles and should be interpreted cautiously.

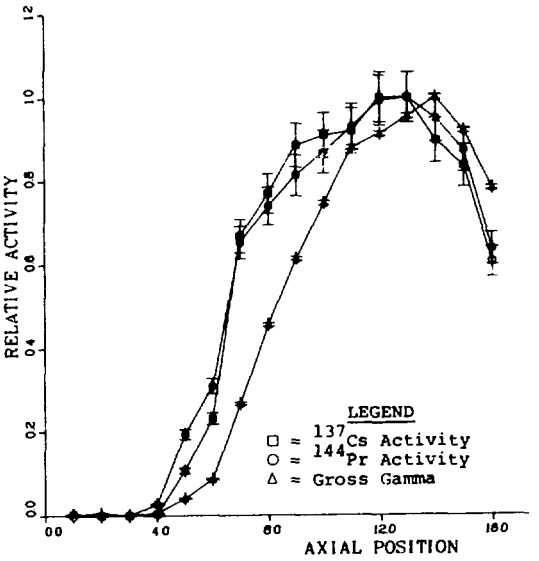

Fig. 11.
Axial profiles for the ^{137}Cs and ^{144}Pr isotopes and the gross gamma activity for the BWR-10 assembly.

Figure 12 shows the relative axial profile measurements of the BWR-10 assembly using the Be(γ,n) results. The Be(γ,n) profile is smoother than the ^{137}Cs profile because the Be(γ,n) detector is uncollimated and therefore "views" a larger segment of the assembly. From this type of analysis, the Be (γ,n) detector appears to give the same general profile as the ^{137}Cs profile for BWR fuel assemblies. To obtain 1% counting statistics, count times between 300-400 s for each axial position were required for a typical assembly. All profiles for the individual isotopic and gross gamma activities are truncated near the bottom of the assembly because if the assembly were raised higher, it would not maintain adequate radiation shielding for personnel at poolside.

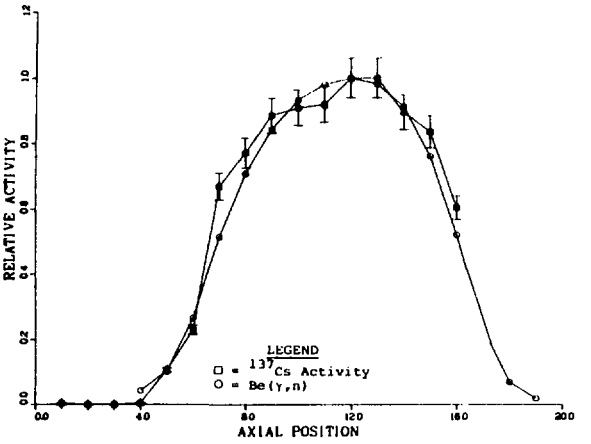

Fig. 12.
Axial profiles for the ^{137}Cs isotope and the Be(γ,n) detector for the BWR-10 assembly.

The ion chamber provided results much more rapidly, requiring only a few seconds to obtain a reproducible measurement ($\sim$1%) at each axial location.[31] The response of the ion chamber depends upon the mixture of energies of the gamma rays reaching the sensitive volume and upon the chamber's sensitivity to each of the energy regions. Detailed calculations have been performed to identify the fission products that contribute significantly to the ion chamber response.[32] The results show that ^{134}Cs, ^{137}Cs, and ^{144}Pr are the principal contributors to the energy deposited in the ion chamber. Figure 13 shows a comparison of the measured ion chamber results with the ^{137}Cs and Be(γ,n) profiles for the BWR-10 fuel assembly. Because the ion chamber was positioned lower than the germanium measurement location, its profile had to be shifted to overlay the other profiles. The advantages of the ion chamber are its rapid response and the short time required to obtain a profile measurement limited only by the operator time needed to move the assembly or the detector.

The relative neutron emission rates were obtained as a function of axial positions by using a small ^{235}U (approximately 10-mg) fission chamber. This detector was also uncollimated, but because the path length of neutrons in

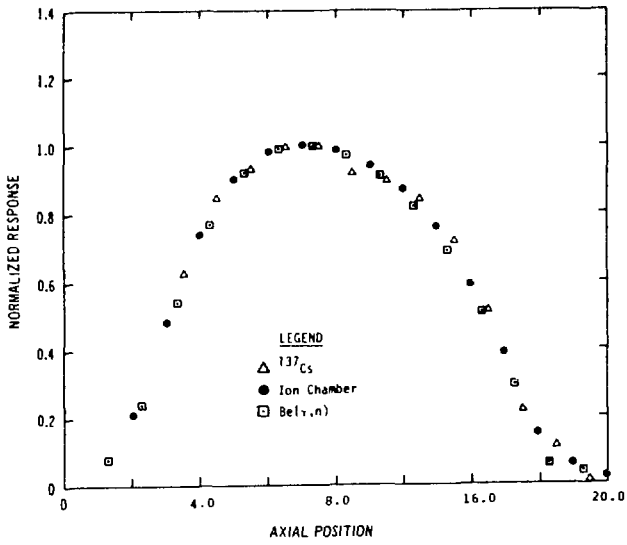

Fig. 13.
Comparison of the activity profiles of BWR-10 using the ion chamber and Be(γ,n) detector to the ^{137}Cs activity profile.

water is small, it measured only the activity of the fuel material at the localized regions. A more detailed discussion of the neutron results is included in Sec. IV.F.

C. Relative Measurement Efficiency for BWR Assemblies as a Function of Axial Position and Between Assemblies

The intrinsic efficiency[13] of the germanium system was calculated at each axial position to determine if the efficiency differed significantly between individual axial positions on the same assembly and if it differed between individual fuel assemblies. The following relationship was used to evaluate the variation of the relative efficiency as a function of gamma-ray energy.

$$\varepsilon = a \cdot \left(\frac{E}{E_0}\right)^b \quad , \tag{14}$$

where

ε = the relative efficiency,

E = the gamma-ray energy,

E_0 = the gamma-ray energy used to normalize the relationship (for ^{134}Cs, E_0 = 604.6 keV), and

a,b = the regression coefficients.

The relative intensities of the ^{134}Cs gamma rays were used to obtain the relative efficiency relationship because the ^{134}Cs covered the energy range from 605 to 1365 keV. This energy range covers all the fission product gamma rays except the 1489- and 2186-keV gamma rays of ^{144}Pr. The relative efficiencies were also calculated for the multiple gamma rays of ^{106}Rh and ^{144}Pr. The variability of the relative efficiencies measured at specific axial positions was within the uncertainty in the counting statistics. Similar results for the intrinsic calibrations were obtained for the ^{106}Rh and ^{144}Pr isotopes. Because we had constant scanning geometry, the efficiencies did not change significantly between individual fuel assemblies. However, we changed the scanning geometry once during these examinations and used this efficiency relationship to normalize the two data sets.

Based upon these results, the net areas for all the full-energy peaks were corrected for differences in the relative efficiencies by using the ^{134}Cs results (605 to 1365 keV) and normalizing to the 604.6-keV gamma-ray line.

The quality of the gamma-ray data is illustrated in Table X, where the uncertainties associated with the counting statistics for various gamma-ray lines

TABLE X

UNCERTAINTIES ASSOCIATED WITH COUNTING STATISTICS

Isotope	Gamma-Ray Energy (keV)	Uncertainty (1σ)
^{134}Cs	604.6	1.9%
	795.8	1.1%
^{106}Rh	622.2	10.1%
	1050.5	12.2%
^{137}Cs	661.6	0.6%
^{144}Pr	696.4	34.6%
	1489.2	10.1%
	2185.6	1.9%
^{154}Eu	1274.4	3.4%
^{88}Y [a]	898.0	2.1%

[a]Yttrium-88 was used as the internal standard to correct for deadtimes and pulse pileup.

are given. For our complete analyses, each line of a specific isotope was correlated with the declared values, but only the results for the best lines are given in the tables.

D. Consistency of Operator-Declared Cooling Times for BWR Assemblies

The declared cooling times of the BWR assemblies ranged from 302 to 1452 days. Consistency of the operator-declared values was determined by using the relationships for single isotopes and isotopic ratios discussed in Sec. II, Eqs. (3) and (4). In this technique, the values of N_i^o and N_i^o/N_j^o must be constant for the set of fuel assemblies, and the relative T_c values must lie on a line defined by the slope $1/\lambda_i$ for single isotopes or $1/(\lambda_j - \lambda_i)$ for isotopic ratios. Any T_c value not lying on this line is inconsistent with the set.

Table XI lists the results for the ^{144}Pr isotope and the $^{106}Rh/^{137}Cs$ and $^{134}Cs/^{154}Eu$ isotopic ratios measured at the midpoint of the fuel assemblies. Most isotopic activities are a function of burnup, and they are not constant for a set of fuel assemblies with different burnups at the time of discharge. However, after a few years irradiation, ^{144}Pr approaches saturation (2-year exposure, 85% saturated) because of its short half-life, in which case it loses its burnup dependence. Also, selected ratios such as $^{106}Rh/^{137}Cs$ and $^{134}Cs/^{154}Eu$ are nearly constant as a function of burnup and, thus, meet the requirement of approximately constant values at time of discharge. In Fig. A-2 in Appendix A, the above activities plotted as a function of burnup show the lack of burnup dependence under these conditions. For example, the ratio of $^{106}Rh/^{137}Cs$ changes by only approximately 3% between 20 000 and 32 000 MWd/MTU. The measured variables for the central four axial positions were summed to give the results in Table XII. These measurements would be expected to have better values because of the associated improvement in the precisions by taking four measurements instead of only one measurement. In this set of fuel assemblies, BWR-1 and BWR-2 (with their very low exposures) do not necessarily satisfy the requirement of constant values at the time of discharge because of having relatively short irradiation periods.

In a typical 3- to 4-year irradiation period of BWR fuel, the ^{144}Pr isotope will approach saturation if the irradiation exposure is relatively constant. Therefore, an inspector can plot the relative ^{144}Pr activities as a function of operator-declared cooling times, and the consistency of the set can be verified quickly.

TABLE XI

COMPARISON OF DECLARED COOLING TIMES AND THE VALUES FROM THE REGRESSION EQUATION[a]

Fuel Assembly	Declared Burnup (MWd/MTU)	Declared Cooling Time (days)	Cooling Times Determined from the Equation[b] (days) ^{144}Pr (2186 keV)	$^{106}Rh/^{137}Cs$ (622/662 keV)	$^{134}Cs/^{154}Eu$ (796/1275 keV)
BWR-1	4 356	842	827	730	--[c]
BWR-2	8 883	1452	1473	1172	1166
BWR-3	13 332	843	771	677	909
BWR-4	14 652	842	1005	1113	1119
BWR-5	15 264	843	802	913	919
BWR-6	16 198	305	459	451	639
BWR-7	16 658	842	881	982	987
BWR-8	17 122	844	983	1049	1126
BWR-9	17 814	842	640	807	938
BWR-10	18 804	302	233	--[c]	382
Average differences			14.8%	15.0%	29.7%

[a]For normal applications, the isotopic ratios are preferable to the single isotopes because ratios are less sensitive to geometric and efficiency factors.

[b]Because this is only a consistency measurement, only the relative cooling time values can be determined.

[c]Insufficient count rate.

TABLE XII

CONSISTENCY OF OPERATOR-DECLARED VALUES FOR COOLING TIMES OF BWR FUEL ASSEMBLIES

Isotope or Ratio		Average Percent Difference
^{144}Pr	(1489 keV)	10.1
	(2186 keV)	7.6
$^{106}Rh/^{137}Cs$	(622/662 keV)	26.4
	(1050/662 keV)	30.6
$^{134}Cs/^{154}Eu$	(605/1275 keV)	33.1
	(796/1275 keV)	20.8

E. Determination of Relative Burnup Values Using Regression Equations for BWR Assemblies

The gamma-ray results were corrected for radioactive decay by using the operator-declared cooling times and then were correlated with the operator-declared burnup values. Operator-declared burnup values have been assumed to be correct within 5% for absolute numbers and about 2% for relative numbers. Calculations were made for the correlations at four axial positions and for their summation. Results for the three measurable parameters having the best correlations with burnup (^{137}Cs, $^{134}Cs/^{137}Cs$, and $^{154}Eu/^{137}Cs$) are given for the four axial positions and their summation in Table XIII. The results for axial position 12 are given in Table XIV with BWR-1 as the major contributor to the average percent difference and showing the lowest burnup value. By excluding BWR-1, the average differences for position 12 drop to 15.8, 17.1, and 8.9%. By combining the results from the four central axial positions, the average differences for ^{137}Cs, $^{134}Cs/^{137}Cs$, and $^{154}Eu/^{137}Cs$ were 16.2%, 19.3%, and 17.9%. The differences indicate that using the maximum activity values gave as good results as taking the sum of several axial positions. The ^{106}Rh isotopic activity correlated with the operator-declared values with an average difference of 24.5% for the summation. The possibility of using a linear combination of two isotopes or isotopic ratios to improve the correlations was explored, but the differences between the results using a single variable and the combinations were not significant.

The assumption of linearity for the $^{134}Cs/^{137}Cs$ and $^{154}Eu/^{137}Cs$ isotopic ratios with respect to burnup may be an oversimplification. For linearity to be true, ^{137}Cs must be directly proportional to burnup and ^{134}Cs or ^{154}Eu must be proportional to the square of burnup. In the following equation, B must be equal to 2.0.

$$^{134}Cs = A \cdot (^{137}Cs)^{B} . \qquad (15)$$

However, for the BWR assemblies, B was determined by fitting the axial profiles of ^{134}Cs and ^{154}Eu each to a power function of ^{137}Cs: 1.60 ± 0.20 for $^{134}Cs/^{137}Cs$ and 1.55 ± 0.20 for $^{154}Eu/^{137}Cs$. Adjusting the ^{134}Cs and ^{154}Eu data to reflect this relationship did not improve the correlations significantly; the average differences for the data at position 12 are 22.7% for $^{134}Cs/^{137}Cs$ and 13.1% for $^{154}Eu/^{137}Cs$. The nonlinear results have slightly larger differences because the function had to go through zero, which was not the case for

TABLE XIII

AVERAGE PERCENT DIFFERENCES BETWEEN THE DECLARED BURNUP VALUES AND THE REGRESSION LINE[a]

Axial Position	Measured Variable: ^{137}Cs	$^{134}Cs/^{137}Cs$	$^{154}Eu/^{137}Cs$
6	27.4% (17.9)	21.6% (17.6)	32.0% (17.2)
8	19.4% (12.6)	27.3% (12.6)	18.7% (16.9)
10	19.5% (12.7)	19.8% (17.0)	20.0% (18.5)
12	18.2% (15.8)	21.4% (17.1)	10.5% (8.9)
Summation (6+8+10+12)	16.2% (13.2)	19.3% (15.2)	17.9% (11.2)

[a]Values in parentheses are average differences obtained without BWR-1 (low burnup) included.

TABLE XIV

COMPARISON OF DECLARED AND MEASURED BURNUP VALUES USING THE REGRESSION EQUATION[a]

Fuel Assembly	Declared Burnup (MWd/MTU)	Burnup Calculated from the Regression Equation (MWd/MTU): ^{137}Cs	$^{134}Cs/^{137}Cs$	$^{154}Eu/^{137}Cs$
BWR-1	4 356	6 099	6 955	3 283
BWR-2	8 883	9 991	10 992	8 708
BWR-3	13 332	10 818	12 171	12 343
BWR-4	14 652	12 418	9 352	11 323
BWR-5	15 264	14 903	15 671	15 665
BWR-6	16 233	16 694	10 546	13 194
BWR-7	16 658	18 398	15 379	16 161
BWR-8	17 122	14 402	13 655	15 947
BWR-9	17 814	15 988	17 238	17 358
BWR-10	18 804	13 425	21 885	21 610
Average difference		18.2%	21.4%	10.5%
Average difference (w/o BWR-1)		15.8%	17.1%	8.9%
Linear correlation[b]: Burnup = a · variable + b				
	Slope a	2 905.19	20 791.19	443 451.6
	Intercept b	1 802.91	-1 630.03	-342.0
	R^2	0.6687	0.6641	0.8997

[a]For normal applications, the isotopic ratios are preferable to the single isotopes because ratios are less sensitive to geometric and efficiency factors.

[b]R^2 is the proportion of the total variation about the mean explained by the regression (Ref. 33). (Appendix C)

the linear model. No corrections were included in either of the above analyses for variation in the irradiation histories between the various fuel assemblies.

F. Neutron Measurements of BWR Fuel Assemblies

The simplicity of the neutron measurement technique makes it particularly attractive for the measurement of irradiated fuel assemblies. Neutrons produced by the spontaneous fissioning of actinide elements and by the (α,n) reaction on ^{18}O can provide a signature that characterizes irradiated materials. The transuranic isotopes that are the principal sources of neutrons in irradiated UO_2 fuel materials are listed in Table B-I in Appendix B.

In a PWR assembly, the interior rods contribute nearly the same amount to the total neutron emission rate as the exterior rods.[21] This advantage and the simplicity of the measurement technique make the neutron signature particularly attractive for characterizing fuel assemblies.

BWR fuel assemblies have been examined to investigate the correlation between declared burnup values and the relative neutron emission rates. Table XV lists measurement results for a set of BWR assemblies with burnup values from 4356 to 17 814 MWd/MTU. All of these fuel assemblies had approximately 840-day cooling times.

The possibility of using a simple power function to relate the measured neutron emission rate and the declared burnup values has been investigated.

$$\text{Neutron counts} = \alpha \cdot (\text{Burnup})^{\beta} \quad . \tag{16}$$

TABLE XV

RELATIVE NEUTRON COUNT RATES AS FUNCTIONS OF AXIAL POSITION

Assembly	Operator-Declared Burnup (MWd/MTU)	Axial Position 6	8	10	12	Summation (6+8+10+12)
BWR-1	4 356	0.095 ± 0.012	0.105 ± 0.012	0.115 ± 0.013	0.107 ± 0.012	
BWR-3	13 332	0.953 ± 0.037	1.273 ± 0.043	1.264 ± 0.042	0.800 ± 0.034	
BWR-5	15 264	3.586 ± 0.072	4.141 ± 0.077	2.656 ± 0.062	0.916 ± 0.036	
BWR-8	17 122	3.900 ± 0.075	5.017 ± 0.085	3.769 ± 0.073	1.317 ± 0.043	
BWR-9	17 814	4.215 ± 0.0788	5.420 ± 0.088	4.308 ± 0.078	2.014 ± 0.054	
Power relationship:		Count rate = α(Burnup)$^{\beta}$				
		β Values				
Burnup: 4 356-17 814		4.32 ± 1.32	4.30 ± 1.08	3.83 ± 0.58	2.41 ± 0.76	3.34 ± 0.76
Burnup: 13 332-17-814		4.41 ± 1.6	4.41 ± 1.25	4.00 ± 0.43	3.22 ± 1.12	3.22 ± 1.12

The values of β determined for two ranges of burnup values range from 2.4 to 4.4 (Table XV). Similar results have been obtained by Fedotov et al[34] for Russian-designed PWR fuels with β = 4.3. The uncertainties of the values are quite large because of the small number of data points which reduces the number of degrees of freedom in the fitting procedure and because of the small range of burnup values. As was noted in Sec. B on axial profiles, the relative neutron profile varies over the length of the fuel assembly and the burnup values supplied by the operator are integral values. Therefore, the ranges of burnup values represented by the four axial positions (6, 8, 10, and 12) should be scaled according to the relative profiles shown in Figs. 11-13. The actual axial positions of the neutron measurements cannot be accurately correlated to the gamma measurements because of the differences in the relative positions of the two detectors.

A comparison of the declared burnup values and the relative burnup values calculated from the regression equation for the four axial positions and the integral is given in Table XVI. Two cases are presented, one with the low burnup value of BWR-1 included and one without. The generally higher average differences in the first case are due to the differences associated with BWR-1. When BWR-1 is excluded from the analysis, the average differences are reduced to less than 5%.

G. Correlation of Destructive Measurements

To understand the relationship between the measured neutron rates and the declared burnup values, an irradiated UO_2 pin from an experimental BWR assembly was destructively analyzed by mass spectrometry and alpha spectrometry to determine the relative concentrations of the actinides[35] as a function of burnup. (The ^{238}Pu listed in Table XVII results from the alpha decay of ^{242}Cm. The destructive analysis did not include an independent measurement of ^{238}Pu; therefore, its contribution to the total neutron emission rate is underestimated because only its production from the alpha decay of ^{242}Cm is considered.) From these measurements, the relative contributions to the total neutron rates for specific isotopes are listed in Table XVII for burnup values ranging from 7400 to 11 450 MWd/MTU and for a cooling time of 2.4 years. The 2.4-year cooling time corresponded to the cooling times of the fuel assemblies measured in Tables XV and XVI. The estimated measurement errors are 0.5% for ^{240}Pu, 12% for ^{242}Cm, and 15% for ^{244}Cm. As can be seen in Table XVII, the neutrons originate

TABLE XVI

COMPARISON OF DECLARED VALUES AND MEASURED VALUES
USING THE REGRESSION EQUATION

Assembly	Operator-Declared Burnup (MWd/MTU)	Value Determined from the Regression Equation — Axial Position 6	8	10	12	Sum (6+8+10+12)
BWR-1	4 356	7 268	7 031	6 787	5 808	6 259
BWR-3	13 332	12 395	12 527	12 690	13 383	12 626
BWR-5	15 264	16 845	16 460	15 405	14 157	16 028
BWR-8	17 122	17 175	17 207	16 864	16 459	17 000
BWR-9	17 814	17 487	17 518	17 479	19 631	17 818
Average difference		17.8%	15.5%	13.0%	11.0%	10.9%
BWR-3	13 332	12 466	12 599	13 036	14 064	12 871
BWR-5	15 264	16 835	16 463	15 696	14 668	16 056
BWR-8	17 122	17 159	17 195	17 131	16 469	16 956
BWR-9	17 814	17 464	17 499	17 713	18 734	17 711
Average difference		4.7%	3.9%	1.4%	4.7%	2.6%

TABLE XVII

PERCENT CONTRIBUTION TO TOTAL NEUTRON RATE
FOR SPECIFIC ISOTOPES AT A COOLING TIME OF 2.4 YEARS

Declared Burnup (MWd/MTU)	Calculated Percent Contribution[a] ^{238}U	^{238}Pu[b]	^{239}Pu	^{240}Pu	^{242}Pu	^{241}Am	^{242}Cm	^{244}Cm
7 400	1.01	0.40	10.26	37.20	1.57	4.10	15.04	30.35
9 760	0.50	0.36	5.84	26.55	1.68	3.48	13.60	47.93
9 840	0.49	0.41	5.33	25.11	1.57	3.85	15.51	47.66
11 450	0.36	0.42	3.8	22.66	1.84	3.42	15.60	51.83

[a]Measured values for specific isotopes can have large errors; the measurement uncertainty of ^{244}Cm can be as large as 15%.

[b]Only the contribution from the alpha-decay of ^{242}Cm; ^{238}Pu was not destructively measured.

primarily from the ^{240}Pu ($t_{1/2}$ = 6570 years) and ^{244}Cm ($t_{1/2}$ = 18.11 years) with the fraction from ^{244}Cm increasing as burnup increases. At the time of discharge, the ^{242}Cm isotope is the dominant contributor to the neutron rate, but has a relatively short half-life ($t_{1/2}$ = 163 days). The longer-lived isotopes, ^{240}Pu and ^{244}Cm, become the dominant contributors at cooling times greater than 2 years.

Figure 14 shows the relative percent contribution to the neutron rate of the various transuranic isotopes as a function of cooling time for the 7400 MWd/MTU fuel sample. For longer cooling times, the relative contribution of ^{240}Pu becomes dominant. As the burnup is increased to 11 450 MWd/MTU (Fig. 15), the relative contributions of the isotopes change significantly. Curium-244 is then the dominant neutron-producing species for burnups above 10 000 MWd/MTU and cooling times greater than two years.

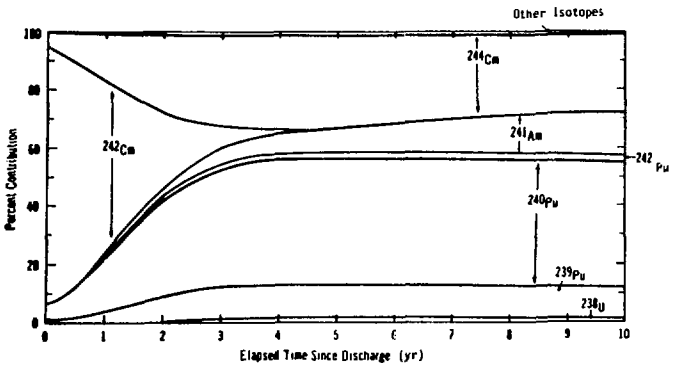

Fig. 14.
Relative percent contributions to the total neutron rate by specific isotopes for a BWR assembly with 7400 MWd/MTU burnup.

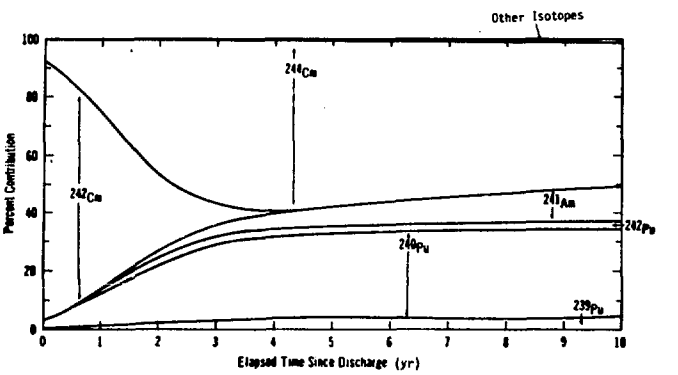

Fig. 15.
Relative percent contributions to the total neutron rate by specific isotopes for a BWR assembly with 7400 MWd/MTU burnup.

V. EXAMINATION OF IRRADIATED PWR FUEL ASSEMBLIES

Fourteen irradiated PWR fuel assemblies were examined nondestructively to evaluate the correlation between gamma-ray and neutron signatures with operator-declared values for fuel burnup (Table XVIII). The burnup values of these assemblies ranged from 16 604 to 32 185 MWd/MTU and the cooling times ranged from 140 to 837 days.

An additional set of 36 irradiated fuel assemblies with burnup values ranging from 18 813 to 38 860 MWd/MTU were measured by using neutron detectors to evaluate the applicability of a simple power function for relating measured neutron response to operator-declared burnup values.

Each fuel assembly consisted of a 15 by 15 array of 204 UO_2 fuel rods with 21 positions for a control cluster and instrumentation guide thimble. The initial ^{235}U enrichment for the fuel was 2.2 to 2.8%. Table XIX lists fuel assembly physical characteristics. The fuel assemblies were irradiated in the Zion Station, Units 1 and 2,* from 1973 (initial criticality) until the dates of discharge listed in Table XVIII. Each unit is rated at 3250 MWt and 1085 MWe.

A. Experimental Techniques

Both gamma-ray and neutron data were acquired on the 14 irradiated PWR assemblies. The detectors were the same as those used in the examination of the BWR fuel assemblies. The scanning arrangement was different because the scanning had to be performed above the storage rack, away from any supporting structure. Figure 16 shows a top view of the scanning arrangement. The fuel assembly was placed in the specified storage location and raised or lowered with the bridge crane for scanning.

The vertical tube was used for the $Be(\gamma,n)$ and neutron detectors, and a separate tube was used for the ion chamber (Fig. 17). The ion chamber used in these measurements was modified to allow its insertion in a 5-cm-i.d. tube (Fig. 18). Its operating characteristics were very similar to the chambers used in the BWR examination and the electronics were identical.

*Operated by the Commonwealth Edison Company.

TABLE XVIII

PWR FUEL ASSEMBLIES EXAMINED NONDESTRUCTIVELY

Fuel Assembly Identification	Initial ^{235}U Enrichment (%)	Declared Burnup Value (MWd/MTU)	Discharge Date	Cooling Time (days)
PWR-1	2.25	16 604	3-76	833
PWR-2	2.25	17 404	1-77	528
PWR-3	2.25	17 776	3-76	832
PWR-4	2.25	18 279	1-77	528
PWR-5	2.25	18 723	3-76	837
PWR-6	2.25	19 826	1-77	524
PWR-7	2.25	19 913	1-77	525
PWR-8	2.25	20 066	1-77	527
PWR-9	2.25	20 252	1-77	527
PWR-10	2.8	29 129	3-78	140
PWR-11	2.8	31 850	9-77	280
PWR-12	2.8	31 851	9-77	278
PWR-13	2.8	32 094	9-77	280
PWR-14	2.8	32 185	9-77	279

TABLE XIX

PHYSICAL CHARACTERISTICS OF PWR FUEL ASSEMBLIES

Fuel geometry	15 by 15 array
Fuel rods per bundle	204 rods with 21 positions for control cluster
Fuel cladding material	Zircaloy-4
Wall thickness	0.062 cm (0.0243 in.)
Diameter of fuel pellets	0.929 cm (0.3659 in.)
Active fuel length	366 cm (144.0 in.)
Enrichment - ^{235}U	2.2-3.3%

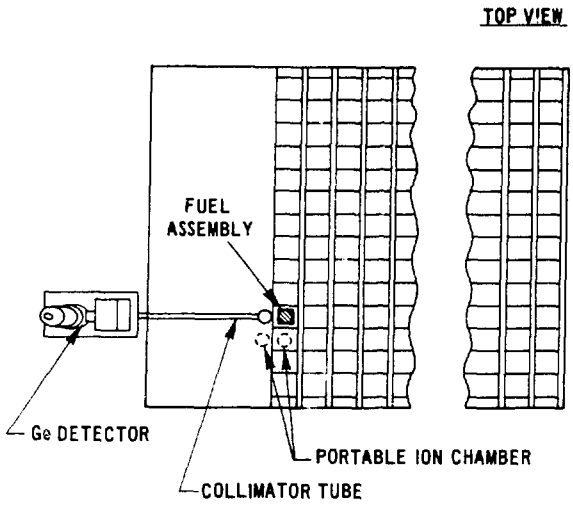

Fig. 16.
Top view of the PWR experimental apparatus showing the relative locations of the detectors.

To obtain axial profile information, the assembly was raised in 30-cm steps with the intrinsic germanium detector recording the gamma-ray spectra, the Be(γ,n) detector measuring gamma-ray intensities more than 1660 keV, the ion chamber determining the gross gamma dose, and the ^{235}U fission chamber measuring the relative neutron flux. Correlations between assemblies were made by comparing the results at a specified axial location.

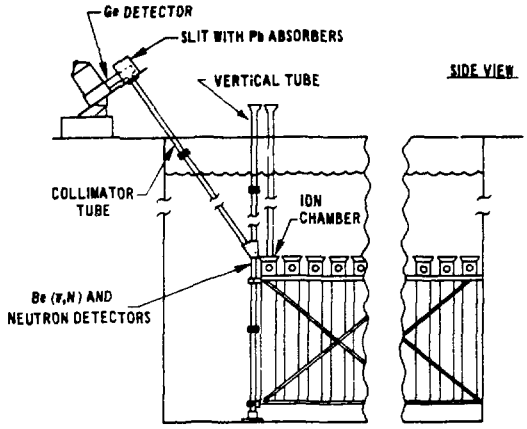

Fig. 17.
Side view of the PWR experimental apparatus.

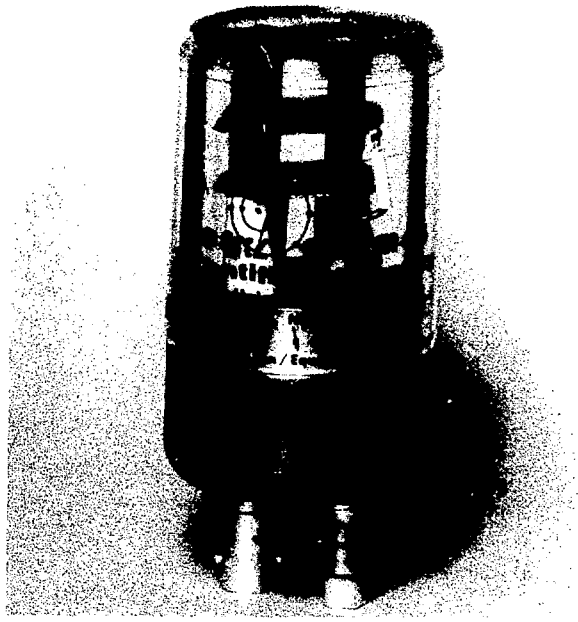

Fig. 18.
The ion chamber used in the PWR examination.

B. Axial Profile Measurements of PWR Fuel Assemblies

As expected, the measured axial activity profiles of PWR fuel assemblies show flatter burnup profiles than those of the BWR fuel assemblies.[36,37] The central fuel regions exhibit similar gamma and neutron emission rates (Figs. 19-21). Figure 19 shows the results of the ^{137}Cs, $Be(\gamma,n)$, and germanium-detector-measured gross gamma axial profiles for the PWR-12 fuel assembly with 31 851 MWd/MTU burnup and 278-day cooling time. The gross gamma profile was obtained by setting a lower threshold ($\sim$200 keV) and summing all the higher energy gamma rays detected in the germanium detector. The agreement between the three profiles is very good.

A similar comparison between the ^{137}Cs profile and the ion-chamber results is shown in Fig. 20. The agreement between these two techniques also is very good. Figure 21 shows the ^{137}Cs and neutron profiles for the same assembly. The neutron measurements were obtained by using an uncollimated fission chamber that was placed adjacent to the fuel assembly. As with the ion chamber results, the neutron profile (Fig. 21) was shifted to coincide with the ^{137}Cs profile because the two detection systems were not physically attached to examine the same axial position. The neutron profile appears to be inside the ^{137}Cs profile as expected because the detector is uncollimated or because the buildup of the transuranic isotopes is less near the ends of the fuel assembly.

C. Relative Measurement Efficiency for PWR Assemblies as a Function of Axial Position and Between Assemblies

The intrinsic calibration[13] of each gamma-ray spectra indicated that the relative efficiency remained constant throughout the examination. The efficiency did not change significantly between various axial positions or between individual assemblies. The ^{134}Cs set of gamma-ray lines was used to correct the spectra for relative differences in efficiencies as a function of gamma-ray energy.

The uncertainties associated with the counting statistics for various gamma rays are shown in Table XX. As in the BWR analysis, all prominent gamma rays from each isotope were correlated with the declared values to allow comparisons.

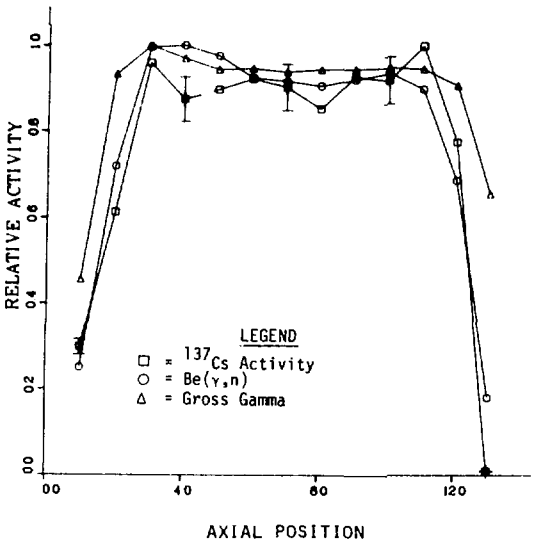

Fig. 19.
Axial activity profiles of the ^{137}Cs, gross gamma activities, and the Be (γ,n) results for the PWR-12 assembly.

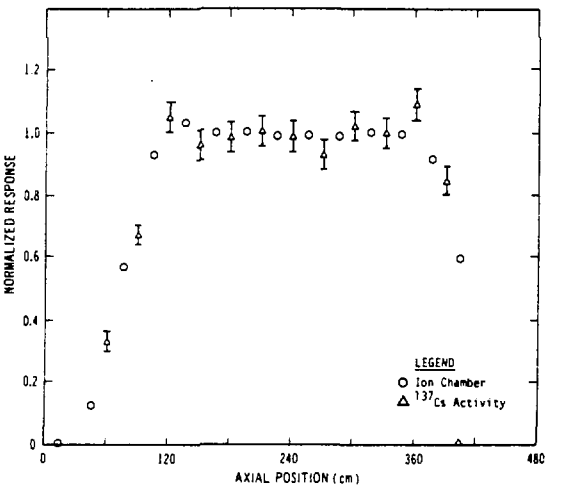

Fig. 20.
Comparison of the axial profiles using the ion chamber with the ^{137}Cs activity profile for PWR-12 assembly.

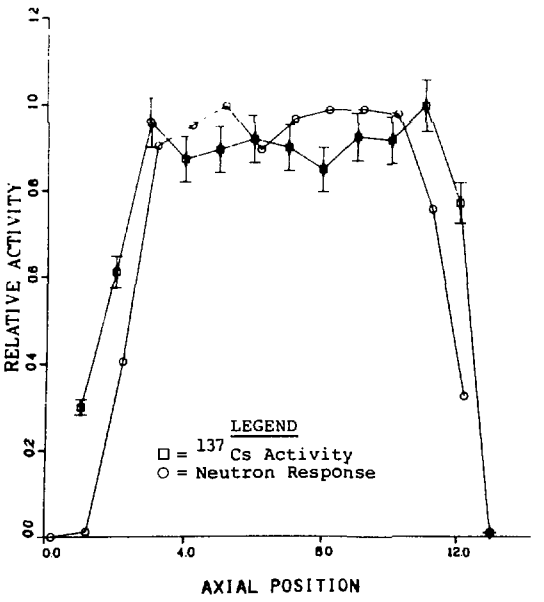

Fig. 21.
Comparison of the axial neutron activity profile with the ^{137}Cs activity profile for the PWR 12 assembly.

TABLE XX

UNCERTAINTIES ASSOCIATED WITH THE COUNTING STATISTICS

Isotope	Gamma-Ray Energy (keV)	Uncertainty (1σ)
^{134}Cs	604.6	6.4%
	795.8	4.2%
^{106}Rh	622.2	6.0%
	1050.5	7.1%
^{137}Cs	661.6	5.0%
^{144}Pr	696.4	17.9%
	1489.2	8.1%
	2185.6	3.5%
^{154}Eu	1274.4	7.9%
$^{65}Zn^{a}$	1115.5	2.9%

[a]Zinc-65 was used as the internal standard to correct for deadtime and pulse pileup.

D. Consistency of Operator Cooling-Time Declarations for PWR Assemblies

Operator-declared cooling times ranged from 140 to 837 days. The consistency of the operator-declared values for cooling times was checked using the techniques that were described in Sec. IV.D for the BWR assemblies. Table XXI lists the results for the individual fuel assemblies at the central axial position of the PWR fuel assemblies. The range of burnups for these assemblies was 16 000 to 32 000 MWd/MTU with exposure periods of 3 to 5 years. The ^{144}Pr isotope from ^{144}Ce ($t_{\frac{1}{2}}$ = 284.5) reaches 93% saturation after only 3 years (this assumes that the flux density is fairly constant throughout the exposure). The ^{144}Pr isotope gave the best correlation with an average difference of 8.1%. It should be kept in mind that these are only relative numbers for cooling time because the consistency of the set of PWR fuel assemblies is being checked. The plotting of relative ^{144}Pr values can also be a rapid check of the differences between relative cooling times. Figure 22 shows a plot of the ^{144}Pr activities as a function of operator-declared cooling times.

Table XXII presents the results obtained by summing the data collected at positions 6, 8, 10, and 12. The ^{144}Pr isotope gave a correlation with an average difference of 7%. For the isotopic ratios investigated, $^{106}Rh/^{137}Cs$ gave the best correlations with an average difference of 11%. The $^{144}Pr/^{137}Cs$ isotopic ratio is often used as a measure of relative cooling times;[11,14] however, for these irradiation periods (2-3 years), the ^{144}Pr would be expected to be saturated and the ^{137}Cs would continue to increase as a function of burnup. Therefore, the ratio would depend upon the burnup.

Isotopic ratios provide the advantage of eliminating correction terms for deadtime and geometrical changes. The $^{106}Rh/^{137}Cs$, and $^{134}Cs/^{154}Eu$ results are also presented in Table XXII. As noted in Appendix A, ^{106}Rh may continue to increase during the irradiation period because of the increasing number of fissions of ^{239}Pu and ^{241}Pu. It also does not begin to become saturated as quickly as the ^{144}Pr (^{144}Ce parent) activity does. If the fission yields for ^{106}Ru from plutonium and uranium isotopes were the same, ^{106}Ru would have become saturated like the ^{144}Pr-^{144}Ce isotope because of the similarity in half-lives (284.5 and 366.4 days for ^{144}Ce and ^{106}Ru, respectively). Therefore, the $^{106}Rh/^{137}Cs$ activity ratio may be a better ratio to measure consistency when irradiation periods are about 3 to 5 years (Fig. 23).

E. Determination of Relative Burnup Values Using Regression Equations for PWR Assemblies

The gamma-ray results from the PWR fuel assemblies gave much better correlations with the operator-declared burnup values than did the BWR fuel assemblies. The uncertainties associated with the operator-declared values were 5% for absolute values and 2% for relative numbers. The data were corrected for radioactive decay by using the operator-declared cooling-time values and correlations were calculated at four axial positions as well as for their summation. The isotope ^{137}Cs and the ratios $^{134}Cs/^{137}Cs$ and $^{154}Eu/^{137}Cs$ correlated well with the declared burnup values. The results for each of the four axial positions and their sums are presented in Table XXIII.

The individual assembly results for position 12 are given in Table XXIV and in Figs. 24-26. The results from single-point measurements have low average differences similar to the results from the summation data.

TABLE XXI

COMPARISON OF DECLARED COOLING TIMES WITH COOLING TIMES DETERMINED FROM THE REGRESSION EQUATION[a]

Fuel Assembly	Burnup (MWd/MTU)	Declared Cooling Time (days)	Cooling Times Determined from the Regression Equation[b] (days)		
			^{144}Pr	$^{106}Rh/^{137}Cs$	$^{134}Cs/^{154}Eu$
PWR-1	16 604	833	829	800	1003
PWR-2	17 404	528	539	541	719
PWR-3	17 776	832	893	717	753
PWR-4	18 279	528	551	541	586
PWR-5	18 723	837	822	699	700
PWR-6	19 826	524	496	514	583
PWR-7	19 913	525	506	506	429
PWR-8	20 066	527	505	546	474
PWR-9	20 252	527	560	524	711
PWR-10	29 129	140	107	182	319
PWR-11	31 850	280	261	347	46
PWR-12	31 851	278	328	319	114
PWR-13	32 094	280	226	321	135
PWR-14	32 185	279	310	339	358
Average difference			8.1%	10.9%	16.0%

[a]For normal applications, the isotopic ratios are preferable to the single isotopes because the ratios are less sensitive to geometric and efficiency factors.

[b]Because this is simply a consistency measurement, only the relative cooling-time values can be determined.

TABLE XXII

CONSISTENCY OF OPERATOR-DECLARED VALUES FOR COOLING TIMES OF PWR FUEL ASSEMBLIES

Isotope or Ratio	Average Percent Difference
^{144}Pr (1489 keV)	6.0
(2186 keV)	8.7
$^{106}Rh/^{137}Cs$ (622/662 keV)	12.8
(1050/662 keV)	9.3
$^{134}Cs/^{154}Eu$ (605/1275 keV)	19.8
(796/1275 keV)	15.1

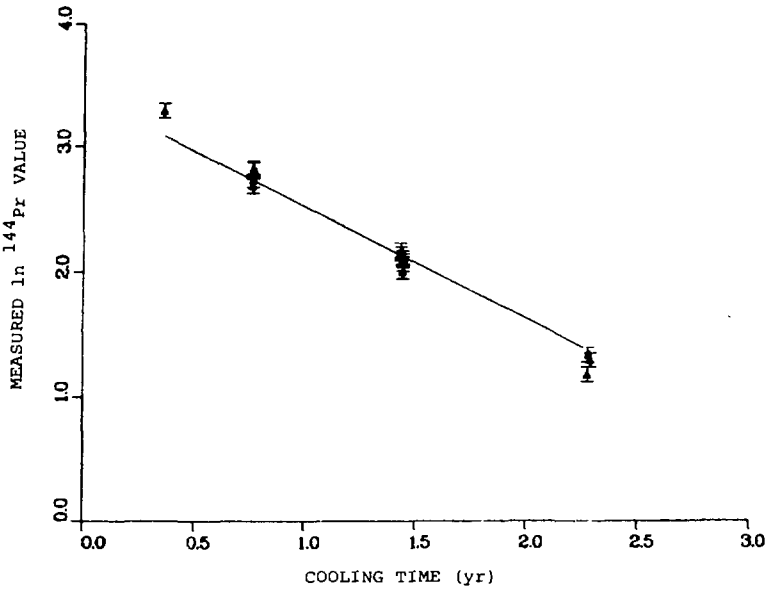

Fig. 22.
Comparison of operator-declared cooling times and ln (^{144}Pr) activities with slope of $1/\lambda$.

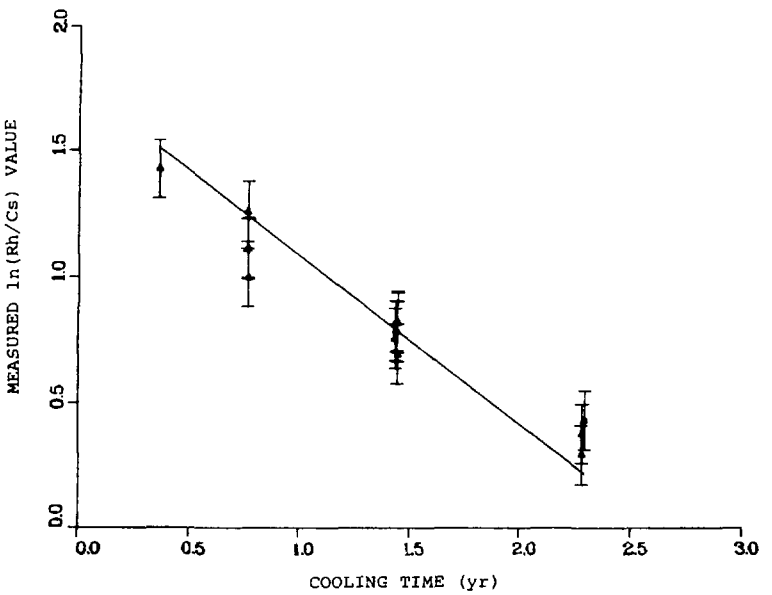

Fig. 23.
Comparison of operator-declared cooling times and ln (^{106}Rh/^{137}Cs) ratios with slope of $1/(\lambda_2-\lambda_1)$.

As discussed in the Sec. IV. on the BWR assemblies, we have used the assumption of linearity for the two ratios over this range of burnup values. The values of B (Eq. 15) were determined from the 14 axial scans to be 1.66 ± 0.18 and 1.74 ± 0.38 for ^{134}Cs and ^{154}Eu, respectively. Adjusting the values of ^{134}Cs and ^{154}Eu improved the average differences only slightly. For position 12, the average differences for the $^{134}Cs/^{137}Cs$ and $^{154}Eu/^{137}Cs$ ratios were reduced to 3.9% and 6.9%, respectively, which are not significantly better than those obtained using the linear model. Therefore, over the ranges of burnup measured in this set of fuel assemblies, a linear model appeared to be satisfactory.

Various linear combinations of isotopes and ratios were investigated to obtain a better predictor of burnup. A partial listing of these combinations is presented in Table XXV. In each of the combinations, either the $^{134}Cs/^{137}Cs$ or $^{154}Eu/^{137}Cs$ ratio is the principal term, and as can be seen from the average differences, the predictability has not been improved significantly by increasing the number of variables.

F. Neutron Measurements of PWR Fuel Assemblies

The 36 irradiated PWR fuel assemblies were examined using two fission chambers, each loaded with ∿130 mg of ^{235}U, oriented 180^{o} opposite each other to minimize the effect of variations in the source-to-detector distance. This geometry was different from that used in the previous neutron measurements. The results from these measurements are given in Table XXVI for 1-minute counting periods taken at the midpoints of the fuel assemblies. Figure 27 shows the data plotted on a log-log plot with no corrections for differences in the cooling times. The 15-20% uncertainty in the measurements is greater than the statistical uncertainty and is due to the difficulty in accurately positioning the detector with respect to the assembly. Four neutron detectors oriented at 90^{o} intervals should be used to obtain better counting geometry. This again emphasizes how critical the source-to-detector distance is in neutron measurements.

The 36 fuel assemblies can be divided into 6 sets using their cooling times. Because the declared burnup values differ by 2-3% within each set, a similar measurement precision would be required to detect any differences within a set. Therefore, with the exception of the 4-month data (counts/time = $\alpha \cdot \text{Burnup}^{\beta}$), all the data were fitted to the simple power function relationship. The regression equation for the data is also plotted in Fig. 27, and

TABLE XXIII

AVERAGE PERCENT DIFFERENCES BETWEEN THE DECLARED BURNUP VALUES AND THE REGRESSION LINE

Axial Position	^{137}Cs	$^{134}Cs/^{137}Cs$	$^{154}Eu/^{137}Cs$
6	8.2%	6.3%	13.4%
8	7.8%	6.3%	12.5%
10	7.3%	6.1%	9.2%
12	4.9%	4.6%	7.9%
Summation (6+8+10+12)	6.4%	5.2%	6.9%

TABLE XXIV

COMPARISON OF DECLARED AND MEASURED BURNUP VALUES USING THE REGRESSION EQUATION[a]

Fuel Assembly	Declared Burnup for Position 12 (MWd/MTU)	Burnup Calculated from the Regression Equation for Axial Position 12 (MWd/MTU)		
		^{137}Cs	$^{134}Cs/^{137}Cs$	$^{154}Eu/^{137}Cs$
PWR-1	16 604	15 313	15 800	15 744
PWR-2	17 404	18 887	16 222	18 299
PWR-3	17 776	17 017	18 338	19 316
PWR-4	18 279	19 298	20 274	17 725
PWR-5	18 723	18 637	19 219	19 397
PWR-6	19 913	19 714	19 110	21 136
PWR-7	19 826	19 694	21 541	22 299
PWR-8	20 066	23 458	20 274	23 054
PWR-9	20 252	19 699	20 328	19 020
PWR-10	29 129	31 099	32 832	30 051
PWR-11	31 850	31 731	30 463	28 659
PWR-12	31 851	30 713	31 050	31 826
PWR-13	32 094	32 094	29 002	23 226
PWR-14	32 185	28 986	31 384	33 582
Average differences		4.9%	4.6%	7.9%
Linear correlation[b]: Burnup = a · Variable + b				
	Slope a	7 799.06	2 5643.61	779 171.41
	Intercept b	-1 868.53	-9 062.48	-14 545.22
	R^2	0.9379	0.934	0.7717

[a]For normal application, the isotopic ratios are preferable to the single isotopes because ratios are less sensitive to geometric and efficiency factors.

[b]The R^2 is defined as the proportion of the total variation about the mean explained by the regression[31] (Appendix C).

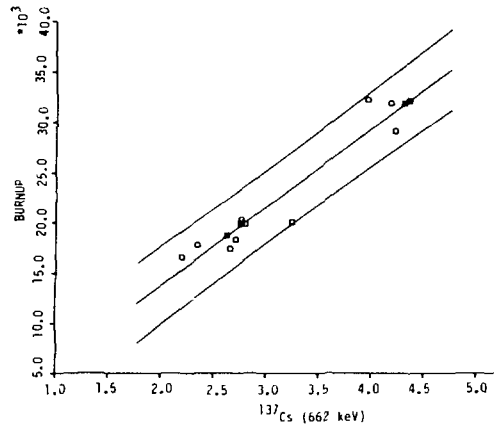

Fig. 24.
Correlation of the measured ^{137}Cs activities with the declared burnup values of the 14 PWR assemblies.

Fig. 25.
Correlation of the measured $^{134}Cs/^{137}Cs$ activities with the declared burnup values of the 14 PWR assemblies.

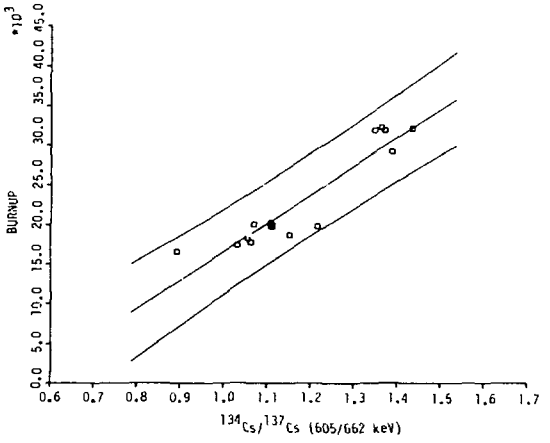

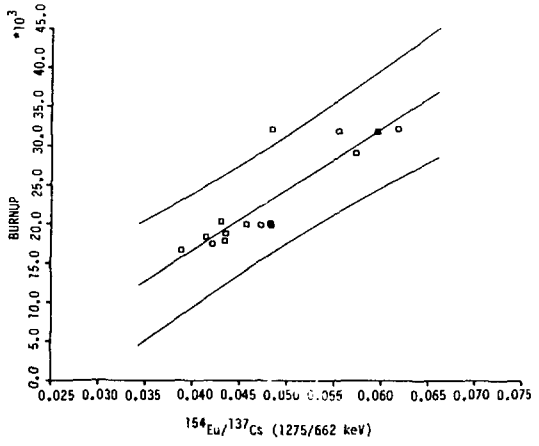

Fig. 26.
Correlation of the measured $^{154}Eu/^{137}Cs$ activities with the declared burnup values of the 14 PWR assemblies.

TABLE XXV

LINEAR COMBINATIONS OF VARIABLES FOR PREDICTING BURNUP VALUES

Variables	Coefficients[a]				Average Percent Difference
	R^2	A	B	C	
$^{134}Cs/^{137}Cs + {}^{154}Eu/^{106}Rh$	0.929	-14 959.6	211 985.7	27 663.8	5.8
$^{134}Cs/^{106}Rh + {}^{154}Eu/^{137}Cs$	0.880	6 300.8	122 267.5	-207 793.4	8.2

[a] Burnup = $A + B \cdot (\text{Variable})_1 + C \cdot (\text{Variable})_2$

the 4-month data lies above the line. This is more clearly illustrated in the linear plot shown in Fig. 28. This deviation from the line probably is due to a high contribution of ^{242}Cm to the total neutron rate (Appendix B). However, in this data set, the burnup values increase as the cooling times decrease, and this can distort the results. Additional measurements are planned to investigate this relationship.

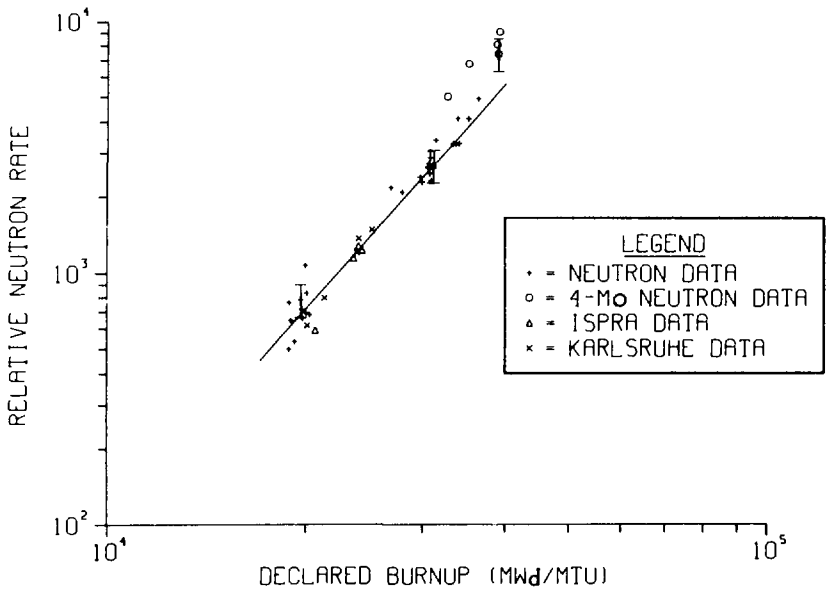

Fig. 27.
Measured neutron ratio vs declared burnup values for 36 PWR fuel assemblies using two fission chamber separated by 180°.

TABLE XXVI

RELATIVE NEUTRON RATES FOR PWR ASSEMBLIES

Fuel Assembly	Initial ^{235}U Enrichment (%)	Operator-Declared Values		
		Burnup (MWd/MTU)	Cooling Time (months)	Neutron Rate (counts/min)
A37P		19 174	40	532
A38P		18 845	↓	762
A39P		18 932	↓	647
A49P		18 813	↓	498
A59R	2.25	19 619	30	781
A58R		19 941	↓	1 078
A57R		19 723	↓	717
A45R		19 728	↓	661
A46R		19 956	↓	694
A47R		20 010	↓	832
A48R		20 223	↓	683
B60R		31 280	22	3 381
B61R		30 551	↓	2 727
B62R		30 546	↓	2 648
B63R		31 080	↓	2 676
B50R		30 836	↓	2 322
B51R		30 668	↓	2 876
B49R	2.80	29 875	↓	2 295
B48R		27 876	↓	2 091
B47R		30 571	↓	2 612
B07P		26 852	17	2 183
B19P		30 665	↓	3 054
B31P		29 699	↓	2 404
B43P		30 675	↓	2 487
B55P		31 070	↓	2 618
C55R		36 278	10	4 929
C57R		33 530	↓	3 263
C58R		33 764	↓	4 133
C59R		33 192	↓	3 273
C47R		33 917	↓	3 287
C48R	3.30	35 055	↓	4 130
C03P		39 025	4	9 132
C15P		38 694	↓	8 110
C39P		35 086	↓	6 773
C51P		38 860	↓	7 427
C63P		32 564	↓	5 026

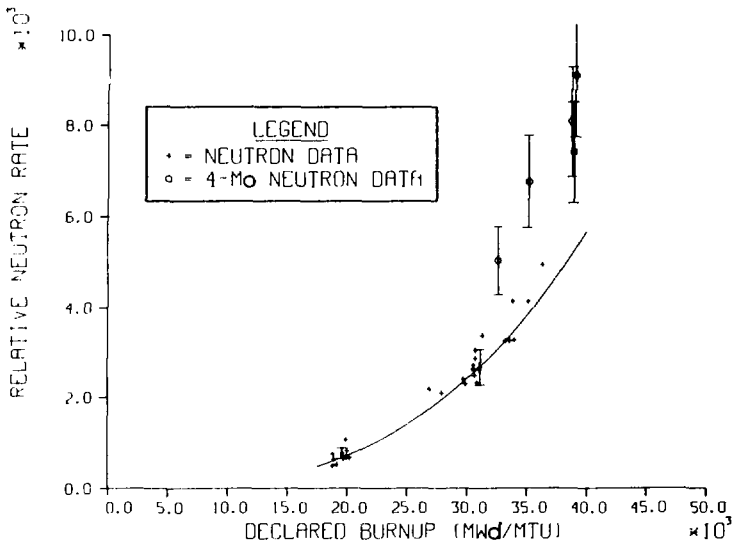

Fig. 28.
Same data as in Fig. 27 but plotted linearly to illustrate that the 4-month cooling times data do not fall on the line.

In Figs. 27 and 28, we have plotted the results from the PWR fuel assemblies without correcting for different cooling times. The results from the destructive analysis of PWR fuel assemblies from the TRINO Reactor, which have a 3-year cooling time, are included for the ISPRA and Karlsruhe results.[38] These data were normalized to 25 000 MWd/MTU. The 3-year cooling time was selected because the PWR assemblies with 20 000 MWd/MTU burnup had similar cooling times.

Figures 29 and 30 show the relative percent contribution to the total neutron rates by the various isotopes from the destructive analysis of TRINO fuel assemblies. The general shapes of the curves are similar, with ^{244}Cm being the principal contributor after a 3-year cooling time. However, the irradiation histories of the TRINO fuel pins were not typical. The exposure had a significant down period (approximately 1100 days) that was similar to Case IV (Appendix B) where the relative contribution of ^{242}Cm was enhanced greatly. The nearly 4-year shutdown would not affect the ^{244}Cm concentration as much as the ^{242}Cm concentration. Therefore, after 1-3 years, one should be able to use the neutron measurement as an indicator of the presence of ^{244}Cm that may be correlated with burnup.

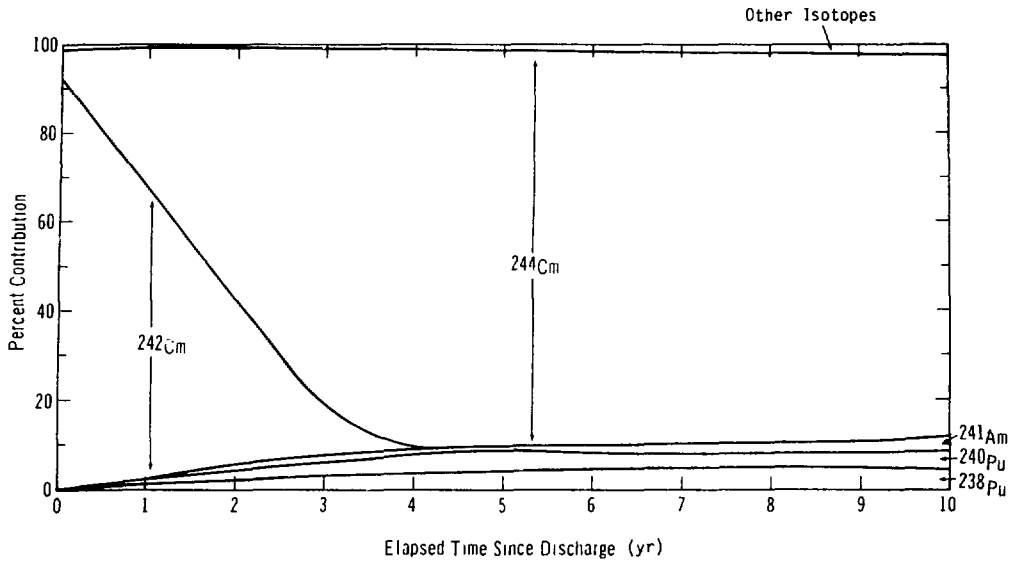

Fig. 29.
Relative percent contributions to the total neutron rate by specific isotopes for a PWR assembly with 20 060 MWd/MTU.

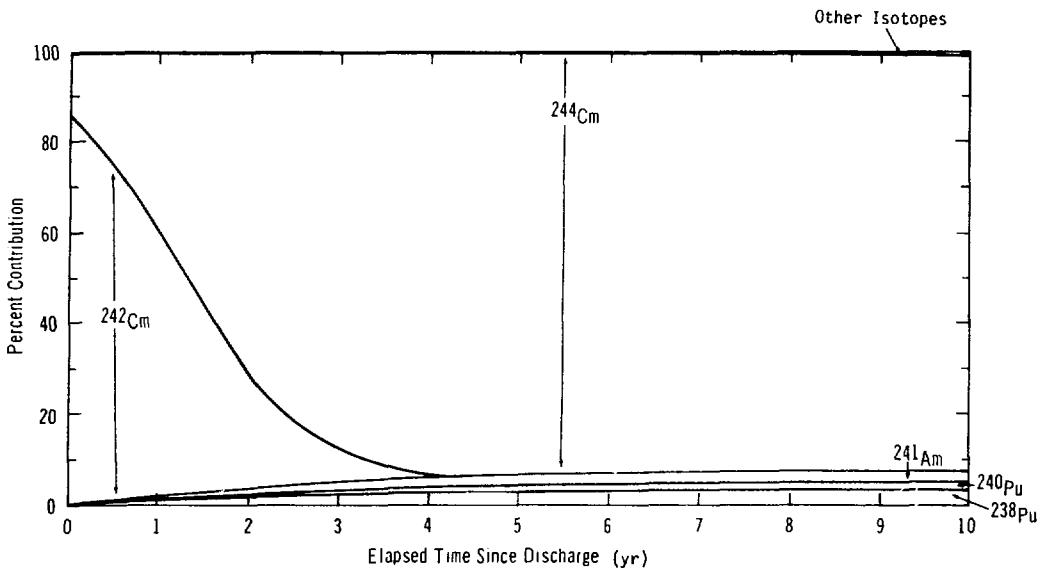

Fig. 30.
Relative percent contributions to the total neutron rate by specific isotopes for a PWR assembly with 25 095 MWd/MTU.

VI. CONCLUSIONS

Various passive gamma-ray and neutron techniques have been applied to the characterization of irradiated LWR fuel assemblies for safeguards. Nondestructive measurements have been correlated with operator-declared values to identify the signatures or combination of signatures that characterize irradiated fuel assemblies. The axial gross gamma activity profile can be measured rapidly by using an easy-to-operate ion chamber. The Be(γ,n) detectors provide more specific fission product profile information, but require longer measurement times. The Be(γ,n) and ion chamber results compare favorably with the ^{137}Cs axial profiles.

The cooling times of irradiated fuel assemblies can be verified only if some irradiation history is available. Techniques like those described in the MTR section (Sec. III) can be used if detailed irradiation histories are available. If no irradiation history is available and only the operator-declared cooling times are available, the consistency of these values can be determined from the measurements. This technique would identify fuel assemblies that do not lie within specified levels of consistency.

Relative burnup values of irradiated MTR, BWR, and PWR fuel assemblies can be measured using HRGS. These techniques may have only limited application to the IAEA inspectors because of the complexity of the instrumentation and hardware. Only the outer regions of the fuel assembly can be examined because of the gamma-ray self-shielding. Even though these disadvantages do exist, this technique is the only one now available for the detailed characterization of irradiated fuel assemblies.

Even though many factors influence the production of ^{134}Cs and ^{154}Eu, the ratios of $^{134}Cs/^{137}Cs$ and $^{154}Eu/^{137}Cs$ gave the best linear correlations for burnup for MTR, BWR, and PWR fuel assemblies. The assumption of linearity between the ratios and burnup should be investigated further for various ranges of burnup values.[39] The use of ratios is preferable to the use of single isotopes because the ratios are less sensitive to geometric and efficiency factors. As in the case for cooling time determination, some information about the irradiation history is required.[16,39]

Passive neutron measurements can provide information about fuel material in the inner regions of the fuel assembly. The relative neutron emission rate depends upon both cooling time and the level of burnup. Other factors that can influence the neutron emission rates are (1) initial enrichment, (2) irradiation history, and (3) flux energy spectra. For assemblies with similar irradiation histories and cooling times, a power function can be used to obtain relative burnup values by using gross neutron measurements.

A single nondestructive measurement can only provide a limited amount of information about irradiated fuel assemblies. By measuring nondestructively several signatures, irradiated fuel assemblies can be characterized more completely. Combining a rapid activity profile with HRGS and neutron measurements at one or two axial positions is probably the most effective safeguards measurement available at the present time. If a lower level of characterization is acceptable, gross gamma and neutron measurements can indicate the presence of irradiated materials, and spectral measurements can identify the presence of fission products. We have evaluated the applicability of a variety of nondestructive techniques for safeguarding irradiated fuel assemblies. The level of confidence of safeguards measurements of irradiated fuel assemblies generally increases as the number of measured characteristics increases where these characteristics are known to correlate with the quantity of fissile material present.

VII. RECOMMENDATIONS FOR ADDITIONAL INVESTIGATION

Our investigation of nondestructive techniques has identified several additional areas in which investigations should be initiated or extended.

1. Applicability of ion and fission chambers for the rapid measurement of irradiated materials. Quantification of gross gamma and neutron signatures with respect to burnup and cooling time may be possible.
2. Calculational modeling of typical LWR fuel assemblies can identify the irradiation parameters that can affect the gamma-ray and neutron signatures directly. Production of ^{134}Cs, ^{154}Eu, and transuranics can be influenced significantly by changes in the neutron spectrum and irradiation history. Calculational modeling can identify which irradiation parameters must be considered in the interpretation of the nondestructive measurements.

3. Sampling is always a problem in any measurement technique. Additional work should be performed to establish how representative measurements on the periphery of an assembly are of the total volume. The physical and chemical properties of the measured isotopes should be investigated to determine their effects upon measurements.
4. Techniques for independent determination of the irradiation histories of individual fuel assemblies should be investigated. Data from reactor power monitors[20] and inspections should be incorporated in the data analysis of passive gamma-ray and neutron measurements to improve the determination of burnup.
5. The present work was limited to burnups in the ranges of 4-18 000 MWd/MTU for BWR assemblies and 16-38 000 MWd/MTU for PWR assemblies, additional work should extend this to the full range of IAEA interest.
6. Because verification of fissile material is a major goal of IAEA inspections, methods to measure directly the fissile content in irradiated fuel assemblies should be pursued.

ACKNOWLEDGMENTS

We wish to thank the various members of the Safeguards Technology and International Safeguards Groups who assisted in these measurements. Special thanks must be extended to the personnel of the Commonwealth Edison Co., Consumers Power Co., and General Electric for their cooperation and support throughout these examinations. The support from the International Safeguards Project Office and the Office of Safeguards and Security is gratefully acknowledged.

APPENDIX A

FISSION PRODUCT PRODUCTION IN LWR FUEL ASSEMBLIES

I. MEASURABLE GAMMA-EMITTING FISSION PRODUCTS

Of the more than 800 fission products produced in irradiated fuel materials, only a few can be measured nondestructively using HRGS. These fission product isotopes are listed in Table A-I. The list has been restricted to measurable fission products with half-lives greater than 30 days.

TABLE A-I

MEASURABLE FISSION PRODUCTS IN LWR FUEL ASSEMBLIES

Isotope	Half-life[40]	Principal Gamma Rays[40-42] (keV)
^{95}Nb	34.97 ± 0.03 days	765.8 (99.82%)
^{103}Ru	39.35 ± 0.05 days	497.1 (86.4%); 610.3 (5.4%)
^{95}Zr	63.98 ± 0.06 days	724.2 (43.1%); 756.7 (54.6%)
^{144}Ce	284.5 ± 1.0 days	696.4 (1.34%); 1489.2 (0.26%); 2185.6 (0.66%). [Gamma rays from ^{144}Pr ($t_{1/2}$ = 17.3 min) daughter].
^{106}Ru	366.4 days	622.2 (9.8%); 1050.5 (1.6%); 1562.2 (0.17%). [Gamma rays from ^{106}Rh ($t_{1/2}$ = 29.8 s) daughter].
^{134}Cs	2.062 ± 0.005 yr	604.7 (97.6%); 795.8 (85.4%); 801.8 (8.7%); 1038.5 (1.00%); 1167.9 (1.81%); 1365.1 (3.04%)
^{154}Eu	8.5 ± 0.5 yr	996.3 (10.3%); 1004.8 (17.4%); 1274.4 (35.5%)
^{137}Cs	30.17 ± 0.03 yr	661.6 (89.9%); [Gamma ray from ^{137m}Ba ($t_{1/2}$ = 2.55 min) daughter].

II. SIMULATED PRODUCTION OF SELECTED FISSION PRODUCTS

A one-point depletion and fission-product computer code, CINDER,[43,44] was used to simulate the production of fission products in a typical BWR assembly. The calculational results indicate the general trends for the build-up of

specific fission products and actinides during a simulated irradiation exposure.[41] The fission-product inventories were calculated for four burnup levels: 8 000, 16 000, 24 000 and 32 000 MWd/MTU. Atomic densities for the eight isotopes listed in Table A-I are plotted for this range of burnup values in Figs. A-1, A-2, and A-3. Figure A-1 shows the saturation of the three isotopes with short half-lives, ^{95}Nb, ^{103}Ru, and ^{95}Zr. The simulated exposure lasted for approximately 4 years to attain a burnup of 32 000 MWd/MTU. The decrease in the relative densities of ^{95}Nb and ^{95}Zr as a function of burnup is related to smaller fission yields from ^{239}Pu fissioning.

In Fig. A-2, ^{144}Pr becomes saturated around 20 000 MWd/MTU burnup for these particular irradiation conditions. Ruthenium-106 increases more rapidly than the ^{137}Cs isotope because the fission yield for ^{239}Pu (4.3%) is higher than for ^{235}U (0.39%). Both the ^{106}Ru and ^{137}Cs atomic densities may be approximated by a linear relationship over normal ranges of burnup. This is particularly true for ^{137}Cs with similar fission yields for both ^{235}U (6.3%) and ^{239}Pu (6.7%) and a relatively long half-life of 30.17 years.

Figure A-3 shows the calculated relative concentration of the ^{134}Cs and ^{154}Eu isotopes as being nonlinear over these burnup values. This nonlinearity can be explained by the mechanisms that produce each of these isotopes. The two ways in which ^{134}Cs can be formed are shown in Fig. A-4. The 134-1 chain yields over 99.9% of the ^{134}Cs produced in this burnup range of 8 000 to 32 000 MWd/MTU. The respective half-lives of the isotopes are enclosed in parentheses with the thermal absorption cross sections given in barns. The ^{133}Cs isotope cross section has resonances in the epithermal neutron region. Variations in the epithermal neutron flux can influence the production of ^{134}Cs.

Formation of ^{154}Eu is more complicated; it is formed as a result of multiple neutron captures by several pathways. These are shown in Figs. A-5, A-6, and A-7. As noted before, the half-lives are enclosed in parentheses and the absorption cross section are given in barns. The samarium isotopes, 149 through 152, all have large cross sections. The relative contributions from each of the three pathways to the total ^{154}Eu atomic density are shown in Fig. A-8 in which the percent contributions for each burnup value are plotted. The contribution from the ^{148}Nd parent chain is dominant throughout this burnup range, whereas the ^{150}Nd parent chain contributes an increasing fraction as the burnup increases.

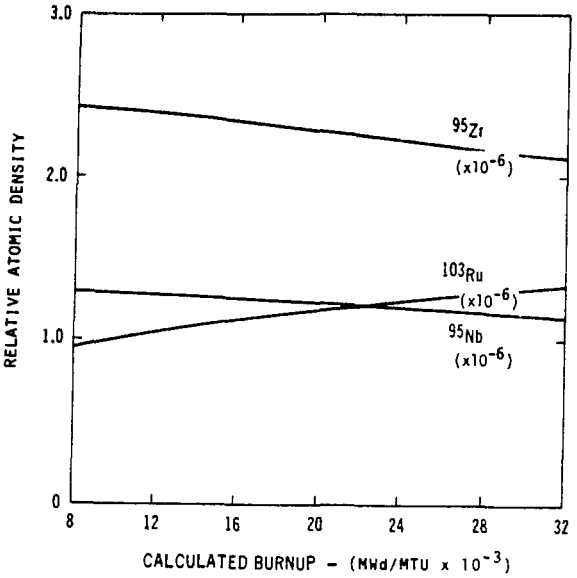

Fig. A-1.
Relative atomic densities of ^{95}Zr, ^{106}Rh, and ^{95}Nb for the burnup range of 8 000 to 32 000 MWd/MTU.

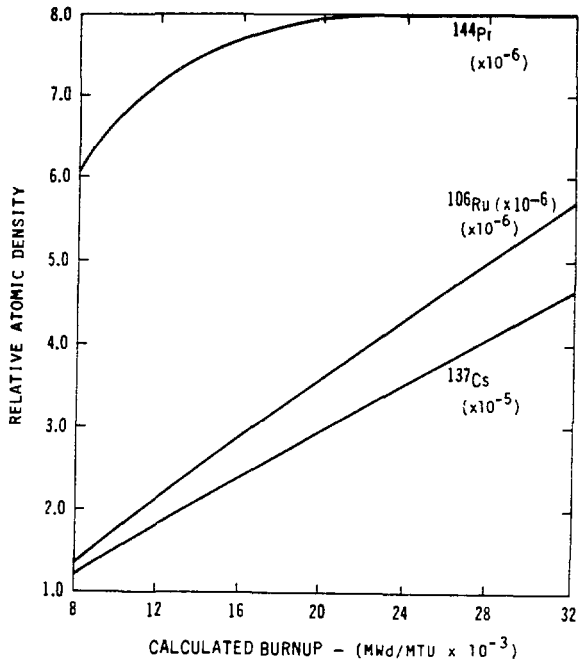

Fig. A-2.
Relative atomic densities of ^{144}Pr, ^{106}Ru, and ^{137}Cs for the burnup range of 8 000 to 32 000 MWd/MTU.

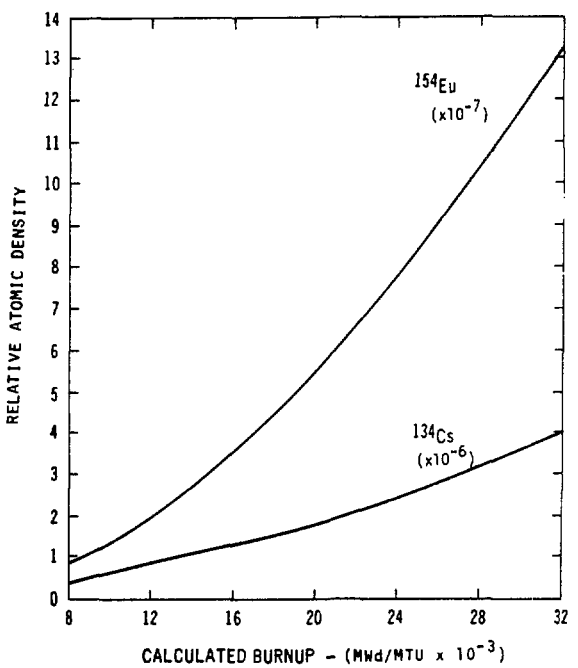

Fig. A-3.
Relative atomic densities of ^{154}Eu and ^{137}Cs for the burnup range of 8 000 to 32 000 MWd/MTU.

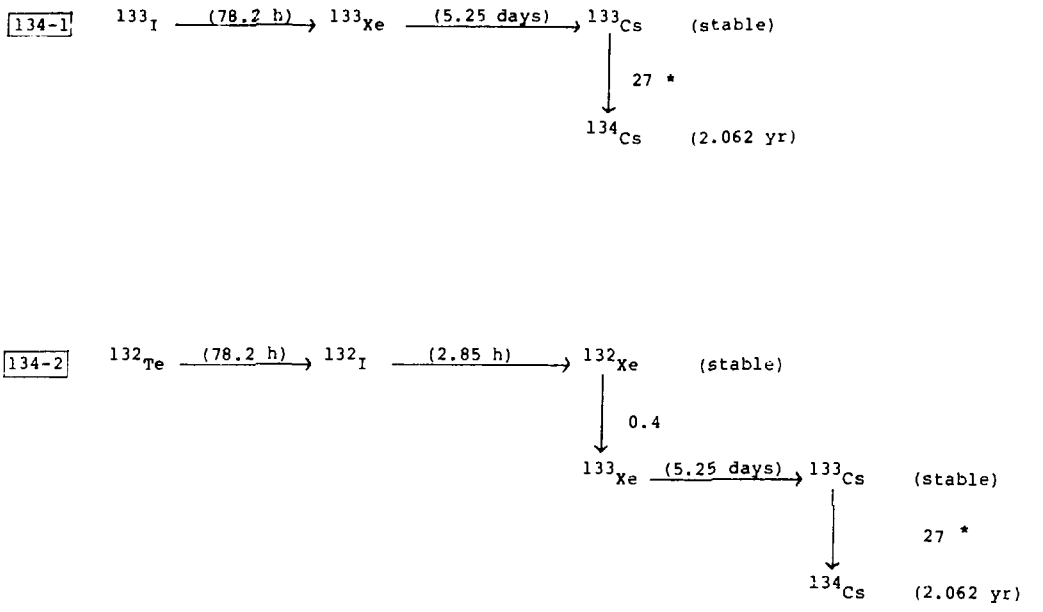

*The resonance cross section can contribute significantly to the production of ^{134}Cs.

Fig. A-4.
Decay chain and production paths for the ^{134}Cs isotope.

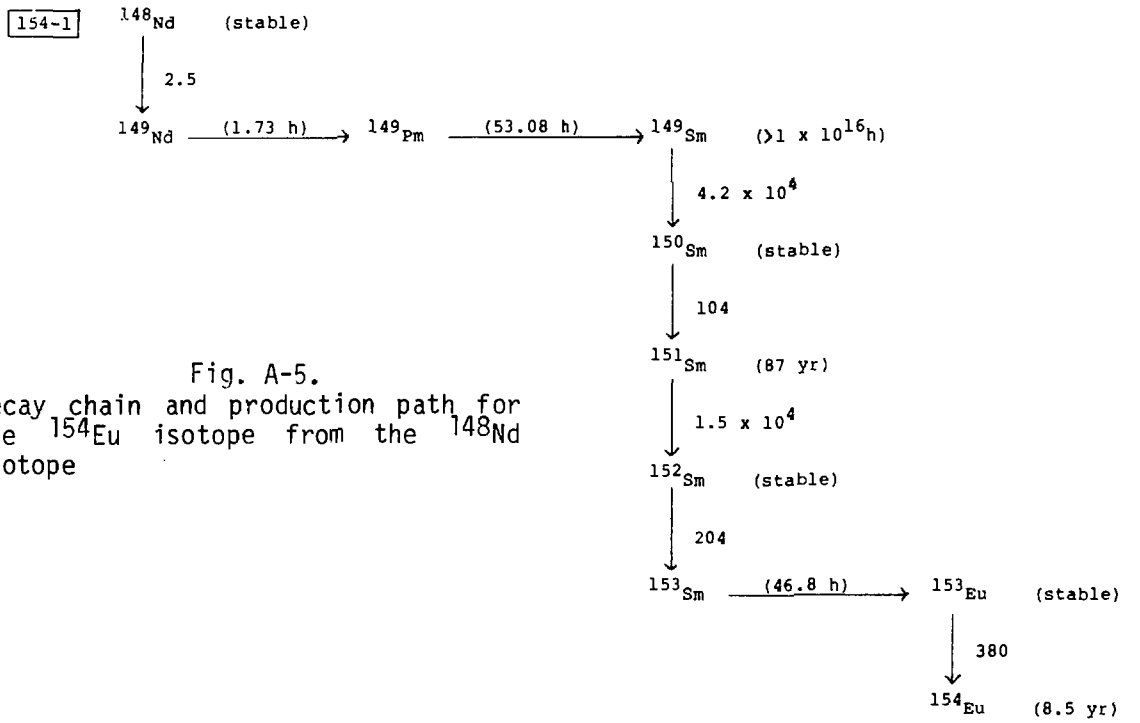

Fig. A-5.
Decay chain and production path for the ^{154}Eu isotope from the ^{148}Nd isotope

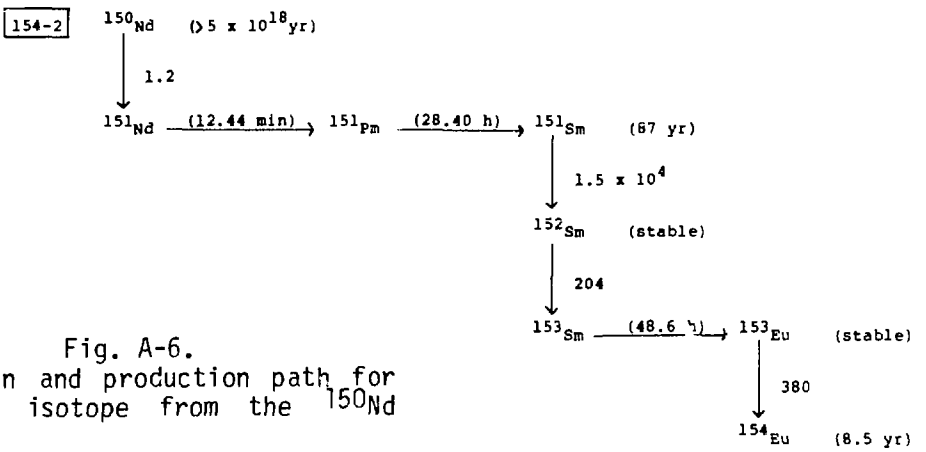

Fig. A-6.
Decay chain and production path for the ^{154}Eu isotope from the ^{150}Nd isotope.

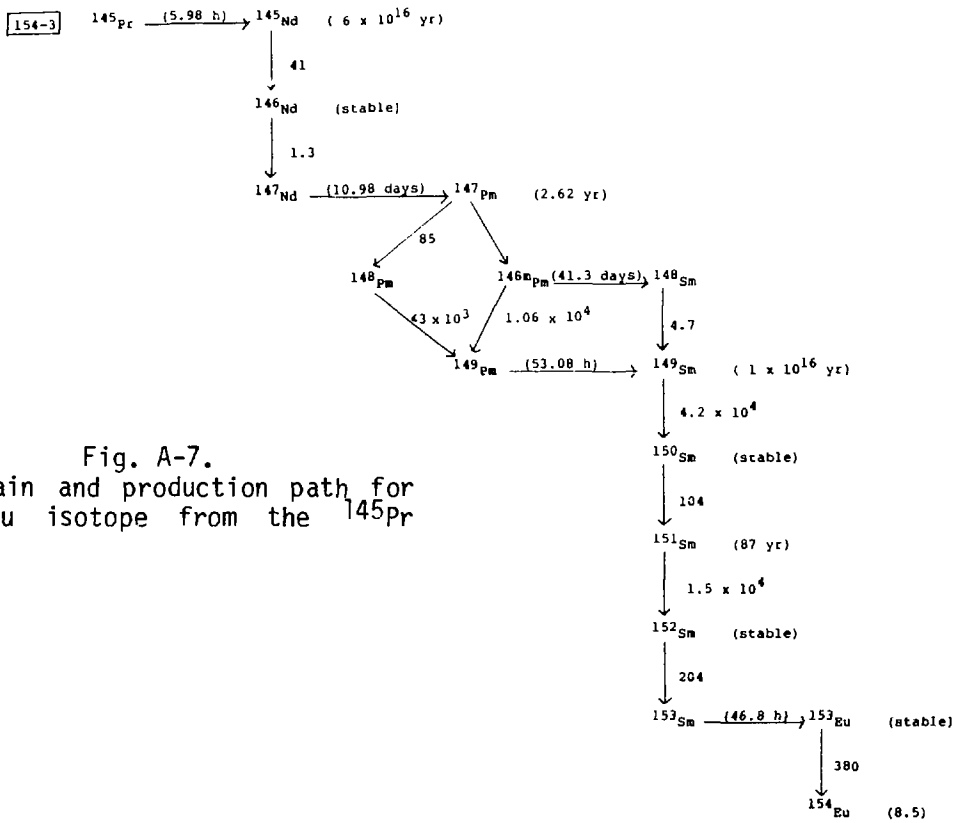

Fig. A-7.
Decay chain and production path for the ^{154}Eu isotope from the ^{145}Pr isotope.

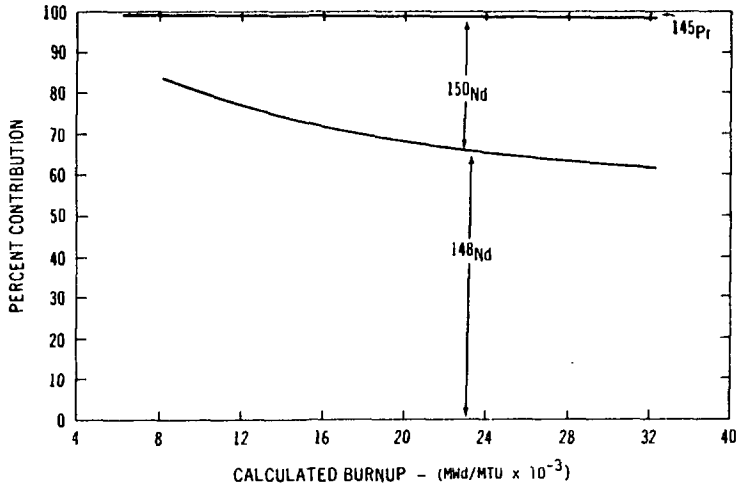

Fig. A-8.

Relative percent contributions to the total ^{154}Eu concentration from ^{148}Nd, ^{150}Nd, and ^{145}Pr as a function of calculated burnup values.

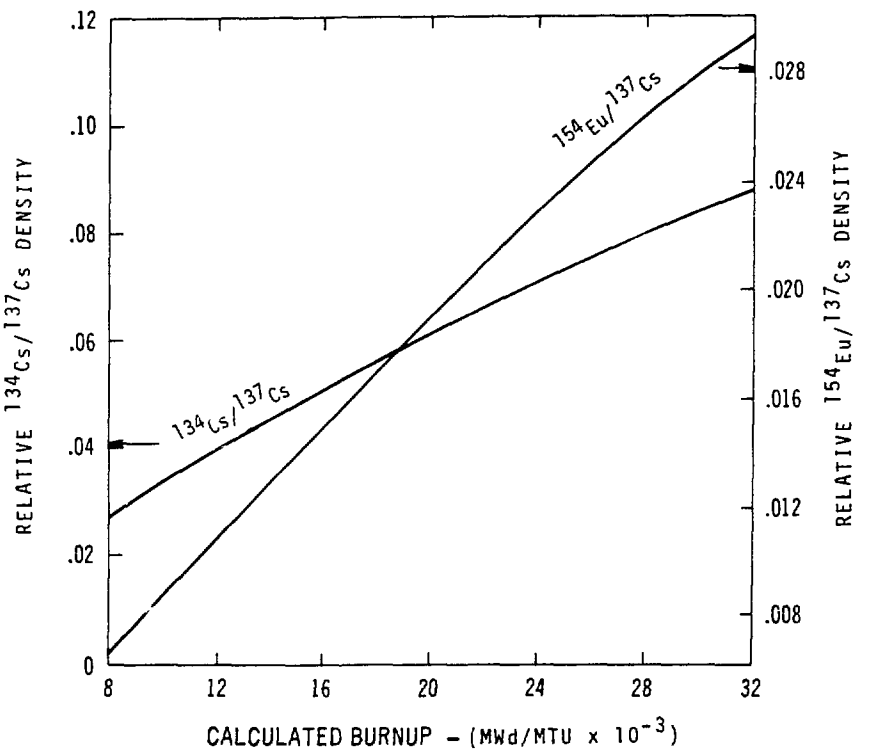

Fig. A-9.

$^{134}Cs/^{137}Cs$ ratios as a function of calculated burnup values.

Many investigators have used a linear relationship between the isotopic ratios $^{134}Cs/^{137}Cs$ and $^{154}Eu/^{137}Cs$ and the burnup of the fuel material. For the BWR test case, the ratios were calculated and are given in Fig. A-9. The relationships are not linear over this range but can be approximated by a linear relationship over specified ranges of burnup. This nonlinear relationship is similar to the values found for the BWR and PWR examinations. This nonlinearity with respect to burnup will be investigated in future calculational and experimental work. Table A-II shows a comparison of the linear approximations to the actual curve. The percent differences should be used only to indicate the approximate values of errors that could be expected from using the linear approximations.

Previous discussions have not considered the problems of measuring the gamma-emitting isotopes listed in Table A-I. Axial and radial migration, resolvability of gamma-ray signatures, and the relative yields of the fissioning isotopes can influence the selection of the *best* fission product or ratios for correlation with reactor physical parameters. Each of the eight isotopes are discussed briefly to identify the advantages and disadvantages of using each.

TABLE A-II

ERROR ASSOCIATED WITH THE LINEAR APPROXIMATION OF BURNUP CORRELATION

Burnup (MWd/MTU)	Burnup $^{134}Cs/^{137}Cs$	Percent Differences	Burnup $^{154}Eu/^{137}Cs$	Percent Differences
8 000	7 314	-8.6	7 552	-5.6
16 000	16 749	4.7	16 302	1.9
24 000	24 559	2.3	24 740	3.1
32 000	31 378	-1.9	31 406	-1.9
	Average	4.4%	Average	3.1%

(1) Niobium-95

$t_{1/2}$ = 34.97 ± 0.03 days.

Principal gamma-ray lines = 765.8 keV.

The majority of ^{95}Nb in irradiated fuels comes from the beta decay of ^{95}Zr. Zirconium-95 produced from the neutron capture of ^{94}Zr can also decay to ^{95}Nb, providing an additional source of ^{95}Nb. Niobium-95 activity becomes saturated relatively easily in the irradiation exposure of typical LWR fuel assemblies. Under certain conditions, ^{95}Nb migrates radially as well as axially in mixed oxide fuel pins.[45-47] Often, the 765.8-keV peak of ^{95}Nb is summed with the 756.7-keV peak of ^{95}Zr as a monitor of the recent fission density of fuel pins. The only significant influence in unfolding spectra for the ^{95}Nb is the 756.7-keV peak of ^{95}Zr, which should not cause any problems with present-day germanium detectors. The fission yield from ^{235}U is 6.5% and from ^{239}Pu is 4.9%.

(2) Ruthenium-103

$t_{1/2}$ = 39.35 ± 0.05 days.

Principal gamma-ray lines = 497.1 and 610.2 keV.

The significant difference in fission yields of ^{103}Ru for ^{235}U (3.0%) and ^{239}Pu (6.8%) explains the increase of ^{103}Ru atomic density at higher burnup values (Fig. A-1). Radial[45] and axial migration of ^{103}Ru has been detected in experimental fuel pins. The 497-keV photopeak is easily resolvable from interferences, whereas the 610.2-keV photopeak can suffer from interferences of ^{137}Cs (604.6 keV) and ^{106}Rh (616.3 keV). Because of the relatively short half-life of ^{103}Ru, it is seldom correlated with parameters for LWR fuel assemblies.

(3) Zirconium-95

$t_{1/2}$ = 63.98 ± 0.06 days.

Principal gamma-ray lines = 724.2 and 756.7 keV.

Zirconium-95 can be used as a monitor for locating the relative position of fuel material as well as the exact locations of interpellet gaps. There

has been no evidence[45-47] that suggests significant radial or axial migration of the isotope. The fission yield for ^{235}U is 6.5% and for ^{239}U is 4.9%; the difference results in a decrease in the atomic density as burnup increases because of the increased contribution of ^{239}Pu fission to the total fissions. This difference in fission yields also explains the slope of ^{95}Nb in Fig. A-1 as ^{95}Zr decays to ^{95}Nb. Both gamma-ray peaks are easily resolvable.

(4) Cerium-144

$t_{\frac{1}{2}}$ = 284.5 ± 1.0 day.
Principal gamma-ray lines = 696.4, 1489.2, and 2185.6 keV from ^{144}Pr daughter.

Cerium-144 has been investigated as a potential burnup monitor because of its half-life, relative chemical inertness, and easily resolvable gamma-ray spectra (^{144}Pr). For long irradiations, the half-life becomes a distinct disadvantage because the ^{144}Ce atomic density reflects the more recent exposure of the fuel assembly (Fig. A-2). Similar effects would be expected for the three previously discussed isotopes. Cerium-144 has been applied as a burnup monitor of CANDU fuels provided certain data are available for a generalized analysis of the reactor and fuel system.[48]

(5) Ruthenium-106

$t_{\frac{1}{2}}$ = 366.5 days.
Principal gamma-ray lines = 622.2, 1050.5, and 1562.2 keV from ^{106}Rh daughter.

The production of ^{106}Rh within irradiated fuel materials is very sensitive to the relative fission rates of ^{235}U and ^{239}Pu. The fission yield for ^{235}U is 0.40% and for ^{239}Pu is 4.3%; therefore, the atomic density of ^{106}Ru increases more rapidly than the corresponding increase in burnup (Fig. A-2). The influence of fission from ^{241}Pu can become significant at higher (~30 000 MWd/MTU) levels of burnup. The fission yield from ^{241}Pu is 6.2%, and with nearly 15% of the fission at 30 000 MWd/MTU being from ^{241}Pu, this effect cannot be ignored.[44] This difference in fission yields can be used to estimate the relative number of fission events in ^{235}U and ^{239}Pu.[49]

Significant radial and axial migration of ^{106}Ru has been detected.[45,47,50] The 512-keV gamma-ray peak of ^{106}Rh has possible interferences from ^{58}Co and annihilation gammas of high-energy gamma-ray lines (>1022 keV). The three lines listed are relatively easy to separate and give three signatures that can be compared to determine any anomalies.

(6) Cesium-134

$t_{1/2}$ = 2.062 ± 0.005 years.
Principal gamma-ray lines = 604.7, 795.8, 801.8, 1038.5, 1167.9, and 1365.1 keV.

Cesium-134 is produced primarily by the neutron activation of ^{133}Cs that comes from ^{133}I through ^{133}Xe; activation is primarily in resonance absorption. Iodine-133 has similar fission yields for ^{235}U (6.8%), ^{239}Pu (6.9%), and ^{241}Pu (6.7%). Therefore, it is relatively independent of the fissioning source. Many examples of radial and axial migration have been detected.[50-53] Migration appears to be a function of a variety of physical and chemical characteristics of the fuel material: thermal gradient, fuel density, and oxygen-to-metal ratio. Cesium-134 appears to migrate more readily than the ^{137}Cs isotope because of the longer half-lives of its precursors ^{133}I and ^{133}Xe. The large number of easily resolvable gamma-ray peaks permits the use of ^{134}Cs to determine the intrinsic efficiency of the detector system under normal conditions.

(7) Europium-154

$t_{1/2}$ = 8.5 ± 0.5 years.
Principal gamma-ray lines = 996.3, 1004.8, and 1274.4 keV.

As was indicated in Figs. A-5 through A-7, the production of ^{154}Eu is very complicated. Europium-154 has essentially no direct production from the fissioning of ^{235}U and ^{239}Pu and results only from multiple neutron absorption of lower mass, high cross-section nuclides. The relative atomic density is nonlinear over the range of burnup values 8 000 to 32 000 MWd/MTU (Fig. A-3). Europium has one of the longest half-lives of the measurable fission products, and it reflects the total irradiation history for typical LWR fuel assemblies.

The isotope does not appear to migrate significantly either radially or axially, but remains uniformly distributed under most irradiation conditions.

(8) Cesium-137

$t_{1/2}$ = 30.17 ± 0.03 years.

Principal gamma-ray line = 661.6 keV (^{137m}Ba).

Cesium-137 has been investigated more than any other fission product because of its easily resolvable gamma-ray and its long half-life. The fission yields for ^{235}U and ^{239}Pu are approximately the same, 6.3% and 6.7%, respectively, with the yield of ^{241}Pu being 6.9%. The only distinct disadvantage of ^{137}Cs is its tendency to migrate radially and axially under certain conditions.[49-51] Often, it is necessary to examine the entire fuel assembly to eliminate the effect of the axial migration. The production of ^{137}Cs in a typical BWR assembly (Fig. A-2) indicates that a linear approximation should be acceptable over typical ranges of burnups and irradiation times.

APPENDIX B

SOURCES OF NEUTRONS PRODUCED IN IRRADIATED LWR FUEL ASSEMBLIES

Irradiated uranium oxide fuel materials emit neutrons that originate primarily from (1) the spontaneous fissioning of transuranic isotopes and (2) the interaction of alpha particles with light materials, in particular ^{18}O. At short cooling times, photoneutron production from the 150-ppm ^{2}H in water can be significant. The principal gamma rays with energy more than 2.2 MeV come from the decay of ^{140}La ($t_{1/2}$ = 40.3 hours), which is in equilibrium with its parent ^{140}Ba ($t_{1/2}$ = 12.8 days). Neutrons produced by these processes can undergo multiplication within the fuel material, thereby producing additional neutrons. The principal isotopes that produce the spontaneous fission neutrons are the even-numbered plutonium and curium isotopes. The transuranic isotopes producing the major fraction of neutrons in irradiated UO_2 material are listed in Table B-I, with the relative contributions from the two processes.

TABLE B-I

PRINCIPAL SOURCES OF NEUTRONS IN IRRADIATED UO_2 MATERIALS

Isotope	Half lives[40] (years)	Neutrons Produced per gram-second: (α,n) Reaction[54-55]	Spontaneous[56] Fission[a]	Total
^{235}U	$7.038 \pm 0.005 \times 10^{8}$	$7.21 \pm 0.72 \times 10^{-4}$	$3.86 \pm 0.99 \times 10^{-4}$	$1.11 \pm 0.12 \times 10^{-3}$
^{238}U	$4.4683 \pm 0.0024 \times 10^{9}$	$8.43 \pm 0.84 \times 10^{-5}$	$1.36 \pm 0.02 \times 10^{-2}$	$1.36 \pm 0.02 \times 10^{-2}$
^{238}Pu	87.71 ± 0.03	$1.56 \pm 0.16 \times 10^{4}$	$2.60 \pm 0.11 \times 10^{3}$	$1.82 \pm 0.16 \times 10^{4}$
^{239}Pu	$2.4131 \pm 0.0016 \times 10^{4}$	$4.25 \pm 0.43 \times 10^{1}$		$4.25 \pm 0.43 \times 10^{1}$
^{240}Pu	$6.570 \pm 0.006 \times 10^{3}$	$1.56 \pm 0.16 \times 10^{2}$	$8.85 \pm 0.10 \times 10^{2}$	$1.04 \pm 0.19 \times 10^{3}$
^{242}Pu	$3.763 \pm 0.009 \times 10^{5}$	2.27 ± 0.23	$1.743 \pm 0.015 \times 10^{3}$	$1.743 \pm 0.015 \times 10^{3}$
^{241}Am	432.0 ± 0.2	$3.17 \pm 0.32 \times 10^{3}$		$3.17 \pm 0.32 \times 10^{3}$
^{242}Cm	0.4456 ± 0.0001	$4.48 \pm 0.45 \times 10^{6}$	$2.25 \pm 0.08 \times 10^{7}$	$2.70 \pm 0.09 \times 10^{7}$
^{244}Cm	18.099 ± 0.015	$8.82 \pm 0.88 \times 10^{4}$	$1.081 \pm 0.007 \times 10^{7}$	$1.090 \pm 0.007 \times 10^{7}$

[a]Reference value for spontaneous fission values.
$\bar{\nu}_{sp} = 3.756$ for ^{252}Cf.

The spontaneous fission contributions were computed using recommended spontaneous fission half-lives[40] and the $\bar{\nu}_{sp}$ values of Manero and Konshin.[56] These $\bar{\nu}_{sp}$ values are referenced to a value of 3.756 ± 0.012 for ^{252}Cf. The uncertainties listed in Table B-I include the contributions from the uncertainties in both the half-life values and the $\bar{\nu}_{sp}$ values.

The production rate of neutrons from the (α,n) reaction of a specific isotope was computed by using a weighted-average alpha-particle energy to determine the neutron yield (n/α) from the results of Bair and Gomez del Campo.[55] These neutron yields were approximately 30-50% higher than the values published by Liskien and Paulsen.[57] However, the higher results agree with values obtained by West and Sherwood[54] for thick targets. The listed uncertainties associated with the (α,n) results are due primarily to large (± 10%) uncertainties in the neutron-yield values. The use of an average alpha-particle energy to compute the reaction cross section will also introduce additional errors.

As can be seen from the isotopes listed in Table B-I, the uranium isotopes initially present in the fuel material, ^{235}U and ^{238}U, are relatively ineffective producers of neutrons when compared to the higher Z isotopes. The transuranic isotopes can be produced by a variety of pathways as illustrated in Fig. B-1.* The relative importance of a particular pathway depends on the irradiation history of the fuel material, including, for example, neutron energy spectra and flow. In Table B-I, for instance, the specific neutron activity of the ^{242}Cm isotope is higher than any of the other isotopes. This isotope is sensitive to the irradiation history of the fuel material because ^{241}Pu is the critical precusor. Plutonium-241 has a half-life of 14.355 $\pm$ 0.007 years for a beta decay to ^{241}Am that then captures a neutron to form ^{242}Am. Americium-242 then beta-decays with a half-life of 16.01 $\pm$ 0.02 hours to ^{242}Cm. The production and sequential decay of the ^{241}Pu isotope is the controlling factor in the production of ^{242}Cm.

To demonstrate this effect, we have simulated various irradiation histories of a BWR fuel assembly by using the single-point depletion code CINDER.[43,44,58] The fuel assembly was restricted to a 2-year irradiation exposure, which resulted in a 16 000 MWd/MTU burnup. The four irradiation histories calculated for the assembly are listed in Table B-II. Case IV, which is atypical for a normal exposure with a 4-year downtime period, is presented for comparisons to the TRINO reactor data.[33] The TRINO reactor was down for an extended period that would significantly change the ^{242}Cm concentration at the time of discharge.

The relative atomic densities of the actinides listed in Fig. B-1 have been determined with their corresponding neutron emission rates. Figure B-2 shows the relative neutron rates for the four irradiation histories as a function of time since discharge. At the time of discharge, the relative neutron rate can vary significantly depending upon the irradiation history; however, after 4- to 5-year cooling times, all four curves combine as a single curve. The relative contribution to the total neutron rate for each isotope is listed in Table B-III for each irradiation history.

*The alpha-decay paths are not shown.

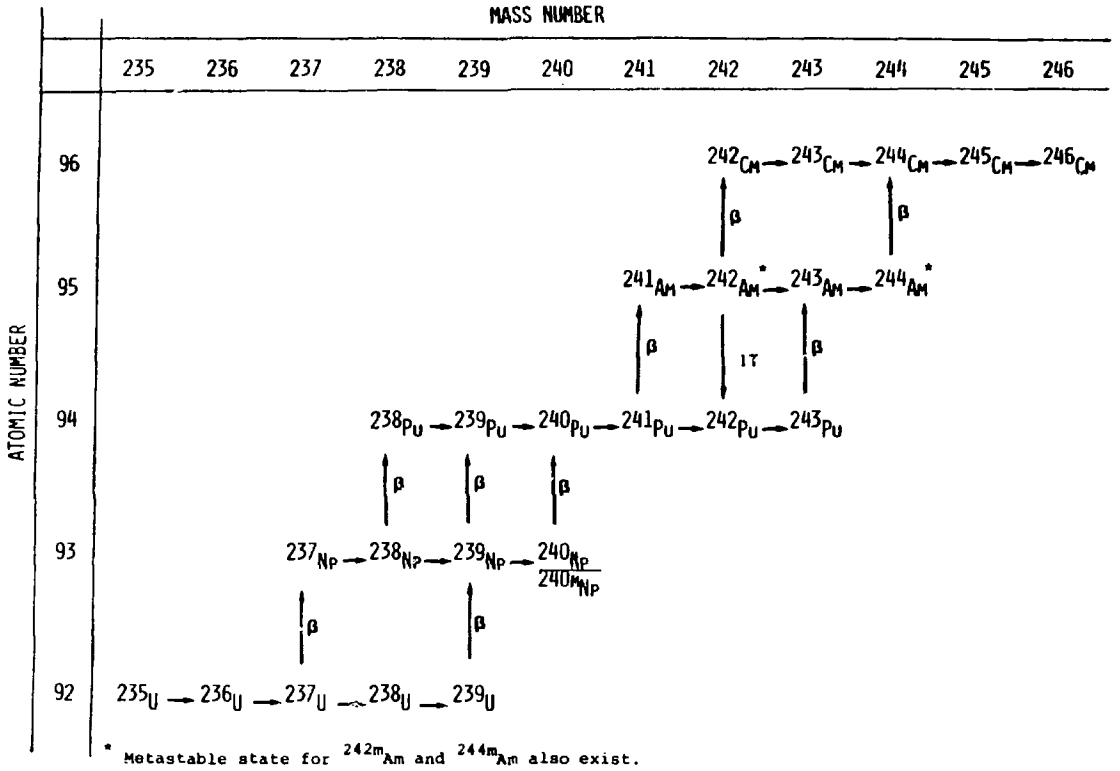

Fig. B-1.
Production chains for the transuranic isotopes from ^{235}U and ^{238}U feed material.

TABLE B-II

SIMULATED IRRADIATION HISTORIES FOR A BWR ASSEMBLY

Case	Initial Irradiation (years)	Shutdown Time	Second Irradiation (years)
I	2	0	0
II	1	50 days	1
III	1	1 years	1
IV	1	4 years	1

During the first 2-3 years, ^{242}Cm, which decays with a half-life of 162.8 days, makes a significant contribution to the total neutron rates. The relative percentage contribution from ^{244}Cm (with a half-life of 18.099 years) increases during this period until it is the dominant neutron-producing isotope for all four irradiation histories. This dependence upon the irradiation history is directly related to the specific beta decay of ^{241}Pu to ^{241}Am as the precursor to ^{242}Cm.

In another set of calculations, four levels of burnup have been simulated by using a relatively constant power level, and the relative concentrations of the actinides have been calculated to determine the relative neutron emission rates. Figure B-3 shows the relative neutron emission rates as a function of time since discharge for burnups that ranged from 8 000 to 32 000 MWd/MTU. The percentage contributions of specific isotopes to the total neutron rate are listed in Table B-IV. As was previously discussed, the ^{242}Cm is the principal contributor at time of discharge. After 4-5 years, its contribution is relatively insignificant, while the relative contribution from ^{244}Cm increases. As the burnup increases, ^{244}Cm becomes the dominant source of neutrons in the range of 3-10 years.

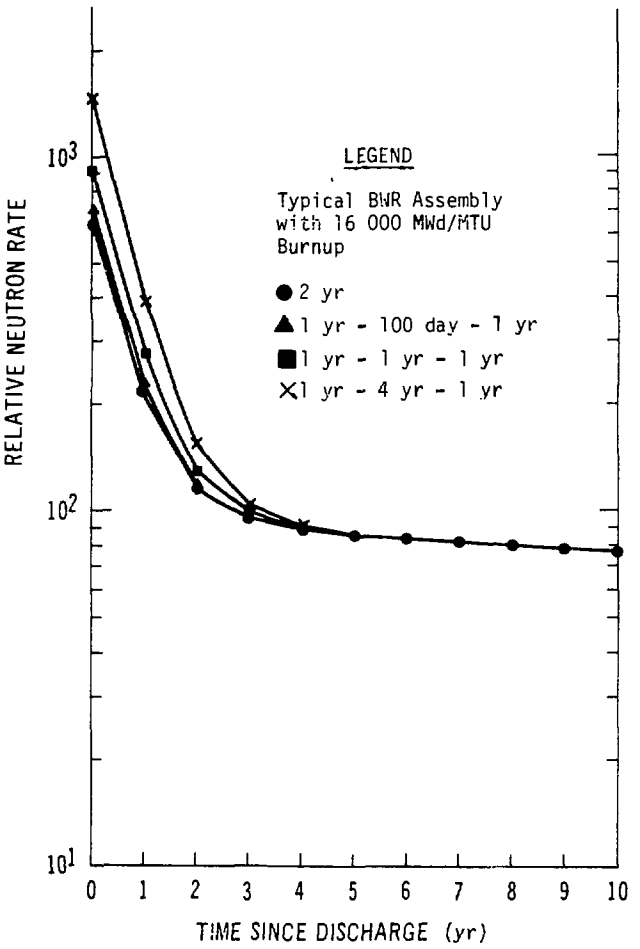

Fig. B-2.
Plot showing the effect of various shutdown periods upon the total neutron rate as a function of cooling time.

The relative neutron emission rate of irradiated fuel material is a function of (1) elapsed time since discharge, (2) total burnup or integrated neutron flux, and (3) irradiation history (in particular, shutdown). Each of these factors has a significant effect upon the relative neutron rates and must be incorporated in the analysis of any neutron measurements of irradiated fuel materials.

These results should be interpreted only as indicating trends. Changes in various reactor physics parameters can affect the relative atomic densities of the transuranic isotopes significantly. A change of 10-20% may be expected in the relative atomic densities for changes in moderator-to-fuel volume, initial ^{235}U enrichment, and fuel-pin diameter.[16] Therefore, comparisons between different reactors should be made only qualitatively. The additional complication is introduced in fuel-shifting management of increasing fuel burnup while minimizing peaking. The production of these neutron-emitting transuranic isotopes is very complicated because of the dependence on so many parameters. However, the neutron-emission rate of an irradiated assembly can provide a signature that is difficult to simulate artificially.

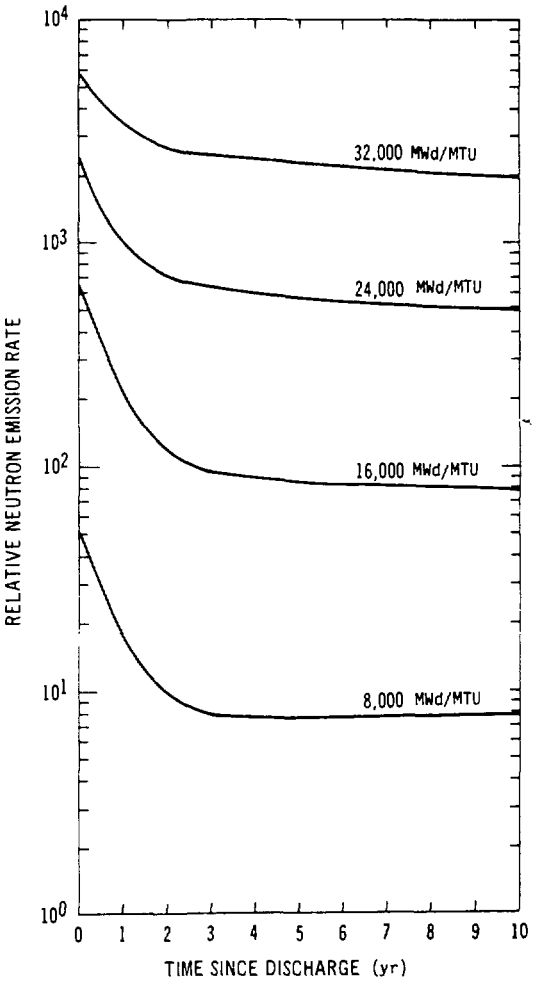

Fig. B-3.
Plots of relative neutron activities as a function of cooling time for four specific burnup values.

TABLE B-III

RELATIVE CONTRIBUTIONS OF ISOTOPES TO THE TOTAL NEUTRON RATES FOR THE FOUR IRRADIATION HISTORIES

Cooling Time (years)	Percent Contribution						
	^{238}Pu	^{239}Pu	^{240}Pu	^{242}Pu	^{241}Am	^{242}Cm	^{244}Cm
No Shutdown							
0	0.5	0.2	1.3	0.2	0.1	85.9	11.8
1	1.8	0.6	4.2	0.6	0.5	56.7	35.6
2	3.3	1.1	7.7	1.2	1.5	22.1	63.2
3	4.1	1.4	9.5	1.4	2.5	5.8	75.3
4	4.3	1.5	10.2	1.5	3.3	1.3	77.8
5	4.6	1.6	10.6	1.6	4.0	0.3	77.5
10	4.8	1.8	11.9	1.8	7.7	0.0	72.1
100-Day shutdown							
0	0.5	0.2	1.3	0.2	0.1	86.6	11.2
1	1.7	0.6	4.0	0.6	0.5	58.1	34.4
2	3.3	1.1	7.6	1.1	1.5	23.1	62.3
3	4.1	1.4	9.5	1.4	2.5	6.1	75.0
4	4.4	1.5	10.2	1.6	3.3	1.4	77.6
5	4.5	1.6	10.6	1.6	4.1	0.3	77.3
10	4.9	1.8	11.9	1.8	7.7	0.0	71.9
One-Year shutdown							
0	0.4	0.1	0.9	0.1	0.1	90.1	8.3
1	1.5	0.5	3.2	0.5	0.4	66.1	27.8
2	3.3	1.0	6.9	1.0	1.4	29.6	56.7
3	4.4	1.4	9.2	1.4	2.5	8.3	72.8
4	4.8	1.5	10.1	1.5	3.3	1.9	76.9
5	4.9	1.6	10.5	1.6	4.1	0.4	76.9
10	5.3	1.8	11.8	1.8	7.7	0.0	71.6
Four-Year shutdown							
0	0.3	0.1	0.6	0.1	0.0	93.5	5.4
1	1.3	0.3	2.3	0.3	0.2	75.7	19.8
2	3.3	0.9	5.8	0.9	0.5	40.4	48.2
3	5.0	1.3	8.8	1.3	0.7	12.9	70.0
4	5.7	1.5	10.1	1.5	0.9	3.1	77.2
5	6.0	1.6	10.6	1.6	1.0	0.7	78.5
10	6.7	1.8	12.4	1.9	1.3	0.0	75.9

TABLE B-IV

RELATIVE CONTRIBUTIONS OF ISOTOPES TO THE TOTAL NEUTRON RATES FOR BURNUP VALUES FROM 8000 TO 32 000 MWd/MTU

Cooling Time (years)	Percent Contribution						
	^{238}Pu	^{239}Pu	^{240}Pu	^{242}Pu	^{241}Am	^{242}Cm	^{244}Cm
8000 MWd/MTU							
0	1.0	1.7	6.4	0.3	0.1	87.2	3.3
1	3.2	5.5	20.3	1.0	1.5	58.4	10.1
2	5.9	10.0	37.2	1.8	4.8	22.5	17.8
3	7.1	12.0	44.5	2.1	8.1	5.7	20.5
4	7.2	12.4	46.0	2.2	10.6	1.2	20.4
5	7.2	12.3	45.8	2.2	12.7	0.3	19.5
10	6.5	11.7	43.5	2.1	20.9	0.0	15.3
16 000 MWd/MTU							
0	0.5	0.2	1.3	0.2	0.1	85.9	11.8
1	1.8	0.6	4.2	0.6	0.5	56.7	35.6
2	3.3	1.1	7.7	1.1	1.5	22.1	63.2
3	4.1	1.4	9.5	1.4	2.5	5.8	75.3
4	4.3	1.5	10.2	1.5	3.3	1.3	77.8
5	4.4	1.6	10.6	1.6	4.0	0.3	77.5
10	4.8	1.7	11.9	1.8	7.7	0.0	72.1
24 000 MWd/MTU							
0	0.4	0.1	0.6	0.2	0.0	73.3	25.4
1	1.1	0.1	1.4	0.4	0.2	37.4	59.3
2	1.7	0.2	2.0	0.5	0.4	11.6	83.6
3	1.9	0.2	2.3	0.6	0.6	2.8	91.5
4	2.0	0.2	2.4	0.7	0.8	0.6	93.2
5	2.1	0.3	2.5	0.7	1.0	0.1	93.3
10	2.3	0.3	3.0	0.8	2.0	0.0	91.5
32 000 MWd/MTU							
0	0.4	0.0	0.3	0.1	0.0	56.3	42.8
1	0.7	0.0	0.6	0.2	0.1	22.0	76.3
2	0.9	0.1	0.7	0.3	0.2	5.8	92.0
3	1.0	0.1	0.8	0.3	0.2	1.3	96.3
4	1.0	0.1	0.8	0.3	0.3	0.3	97.2
5	1.1	0.1	0.8	0.3	0.3	0.1	97.3
10	1.3	0.1	1.0	0.4	0.6	0.0	96.6

APPENDIX C

STATISTICAL TECHNIQUES USED IN EVALUATION PROCESS

I. SELECTION OF PARAMETERS

The objective of the statistical analyses of the measured parameters was to determine what variable or group of variables provided the best prediction of relative cooling time and burnup values. The variables that were investigated included the specific activities of fission products and ratios of activities.

One of the criteria used to select a predictor (or set of predictors) is the squared simple (or multiple) correlation coefficient R^2. This quantity is expressed as

$$R^2 = \frac{\sum(\hat{Y}_i - \overline{Y})^2}{\sum(Y_i - \overline{Y})^2} \quad ,$$

where $\hat{Y}_i$ is the ith observation, $\overline{Y}$ is the mean of the $\hat{Y}_i$'s and Y_i is the estimated value obtained from the regression equation. The R^2 is the proportion of the total variation about the mean $\overline{Y}$ explained by the regression.[33] It is often expressed as a percentage by multiplying by 100.

This selection criterion is used to indicate variables that from a statistical point of view explain the variation in the dependent variable. These results must be incorporated with knowledge of the physical and chemical properties of the variables to select the set of variables that can best correlate with declared cooling time and burnup values.

II. MULTIVARIATE TECHNIQUES[59]

Multivariate techniques were used to determine if the set of variables could be subdivided into smaller groups. Such groupings could be useful for two reasons. The first is to assure that variables containing information not present in any other variables are not arbitrarily excluded from consideration in the prediction equation. Second, if such groupings could be achieved, it might not be necessary to use more than one variable from a group in a prediction equation. However, variables that do not fall in a well-defined group

might offer unique information concerning the dependent variables. It is also possible that such predictor variables simply contain information that is contained in two or more of the other groups of variables.

The procedures used to examine the multivariate structure of the peaks and ratios were principal component analysis and cluster analysis. Principal component analysis was used to determine the number of space dimensions required to contain most of the variation in the independent variables. Each dimension is a linear combination of the variables and is not necessarily a specific variable. If it is determined that most of the variation in the predictor variables is confined to a small number of dimensions (possibly two or three), it may be possible to separate these variables into groups with different information content. Ideally, one would like the information content of all groups to be mutually exclusive and exhaustive. However, this can seldom be achieved in practice.

Cluster analysis was used as an exploratory technique to search for groupings of the predictor variables. From the principal component analysis, we determined that most of the variation in the predictor variables was confined to a small number of dimensions. Cluster analysis provided a qualitative method of grouping variables that would provide similar information. Selecting one variable from each grouping could provide sufficient information, but if we had selected two variables from a single grouping, we probably would not have increased significantly our total information about the dependent variable. Functionally, we were attempting to obtain a relationship between a minimal number of measured variables and relative cooling times or burnups of individual assemblies. This can be illustrated by

$$\text{Declared Value} \propto f(C_1, C_2, C_3, \ldots) \quad , \tag{B.1}$$

where C_1 is a variable from the ith cluster. A cluster can consist of a single variable and that would imply the variable could provide unique information with respect to the dependent variable (cooling time or burnup).

III. APPLICATION OF RESULTS

This analysis can be of particular importance in the selection of combinations of variables to be used for establishing correlation with measured values that improve detection probability. Any isotopic ratio will have zero sensitivity to certain types of diversion scenarios; this zero sensitivity is called a "blind spot." Methods for identifying and compensating for blind spots in the isotopic ratio require the solution of a system of equations. These equations predict the possible combinations of overall isotope changes that will produce no response in the isotopic ratios being used. The use of a number of distinct ratios that is greater than the number of isotopic concentrations that the diverter may conceivably manipulate ensures that the blind spots to diversion are covered. Only two or three ratios may be required in practice because other constraints may eliminate many mathematically possible but practically impossible diversions.

The statistical procedures described here were used to provide supplementary information to aid in the selection of variables based upon physics. They were not used with the intention of providing conclusive results and, in fact, could not have done so with the relatively small sample sizes available. They did, however, make it possible to reveal patterns of relationships among a large number of variables that might otherwise not be evident.

REFERENCES

1. "IAEA Safeguards Technical Manual: Introduction, Part A, Safeguards Objectives Criteria and Requirements," International Atomic Energy Agency report IAEA-174 (1976).

2. S. C. T. McDowell, "Safeguards and Nonproliferation," in Analytical Methods for Safeguards and Accountability Measurements of Special Nuclear Materials, H. T. Yolken and J. E. Ballard, Eds., Proc. Am. Nucl. Soc. Top. Meet., Williamsburg, Virginia, May 15-17, 1978, NBS Publication 528.

3. D. D. Cobb, H. A. Dayem, and R. J. Dietz, "On Safeguarding Spent Nuclear Fuels," Los Alamos Scientific Laboratory report LA-7730-MS (June 1979).

4. "The Structure and Content of Agreements Between the Agency and States Required in Connection with the Treaty on the Nonproliferation of Nuclear Weapons," Vienna, International Atomic Energy Agency report INFCIRC/153, (June 1972).

5. T. Haginoya, M. Ferraris, W. Frenzel, I. Kiss, F. Klik, V. Poroykov, L. Thorne, and S. Thorstensen, "Experience in the Application of Agency Inspection Practices," in Nuclear Safeguards Technology 1978, Symp. Proc. Int. Symp. Nucl. Mater. Safeguards, Vienna, October 2-6, 1978, International Atomic Energy Agency report IAEA-SM-231/105, Vol. I., pp. 3-9.

6. "Nonproliferation and International Safeguards," International Atomic Energy Agency report IAEA-575 (1978).

7. C. W. Alexander, C. W. Kee, A. G. Croff, and J. O. Blomek, "Projections of Spent Fuel to be Discharged by the U.S. Nuclear Power Industry," Oak Ridge National Laboratory report ORNL/TM-6008 (October 1977).

8. "Program for Technical Assistance to IAEA Safeguards - Second Program Plan," Dept. of Energy (June 1, 1978).

9. R. R. Edwards, "A Review of Recent Studies of Nondestructive Assay Methods for Irradiated Nuclear Fuels," Nucl. Appl. Technol. 4, 245 (April 1968).

10. T. Dragnev, "Nondestructive Assay Techniques for Nuclear Safeguards Measurements," At. Energy Rev. 11, No. 2, (1973).

11. S. T. Hsue, T. W. Crane, W. L. Talbert, Jr., and J. C. Lee, "Nondestructive Assay Methods for Irradiated Nuclear Fuels," Los Alamos Scientific Laboratory report LA-6923 (January 1978).

12. International Atomic Energy Agency Advisory Group Meeting on the Nondestructive Analysis of Irradiated Power Reactor Fuel, AG-11, Vienna, April 1977.

13. T. N. Dragnev, "Intrinsic Self-Calibration of Nondestructive Gamma Spectrometric Measurements," International Atomic Energy Agency report IAEA/STR-60 (1976).

14. A. J. G. Ramalho and W. E. Payne, "Spent Fuel Measurements Using High-Resolution Gamma Systems," Nucl. Mater. Manage. VIII, 76 (Fall 1979).

15. P. Brand, A. Cricchio, and L. Koch, "Feasibility Study of the Use of Radioactive Fission Product Correlations for the Determination of Burnup and Heavy Isotopes Composition of BWR Dodewaard Fuel," Joint Nuclear Research Centre report EUR-4909e (1972).

16. E. H. Ottewitte, "Evaluation of Analytical Capabilities for Accurate Prediction of Isotopic Correlation Ratios," Idaho National Engineering Laboratory report RE-P-77-044 (June 1977).

17. E. P. Blizard, editorial, Nucl. Sci. Eng. 9, No. 3 (1961).

18. T. R. England," An Investigation of Fission Product Behavior and Decay Heating in Nuclear Reactors," U. of Wisconsin, Ph.D dissertation (August 1979).

19. N. Beyer, M. deCarolis, E. Dermendjiev, A. Keddar, and D. Rundquist, "IAEA NDA Measurements as Applied to Irradiated Fuel Assemblies," in Nuclear Safeguards Technology 1978, Symp. Proc. Int. Symp. Nucl. Mater. Safeguards, Vienna, October 2-6, 1978, International Atomic Energy Agency report IAEA-SM-231/101, Vol. I, pp. 443-457.

20. E. J. Dowdy, A. A. Robba, R. B. Hastings, and S. W. France, "New Instrument for the Confirmation of Declared Power Histories of Central Station Nuclear Power Plants," Nucl. Mater. Manage. VIII, 689-707 (Fall 1979).

21. S. T. Hsue, J. E. Stewart, K. Kaieda, J. K. Halbig, J. R. Phillips, D. M. Lee, and C. R. Hatcher," Passive Neutron Assay of Irradiated Nuclear Fuels," Los Alamos Scientific Laboratory report LA-7645-MS (February 1979).

22. H. O. Menlove, Los Alamos Scientific Laboratory, private communication, June 1979.

23. J. R. Phillips, T. R. Bement, K. Kaieda, and E. G. Medina, "Nondestructive Verification of Relative Burnup Values and Cooling Times of Irradiated MTR Fuel Elements," Los Alamos Scientific Laboratory report LA-7949-MS (August 1979).

24. H. T. Williams, A. R. Lyle, D. W. Stopinski, C. L. Warner, J. L. Yarnell, and H. L. Maine, "1969 Status Report on the Omega West Reactor with Revised Safety Analysis," Los Alamos Scientific Laboratory report LA-4192 (July 1969).

25. S. T. Hsue, C. R. Hatcher, and K. Kaieda, "Cooling Time Determination of Spent Fuel," Nucl Mater. Manage. VIII, 356-367 (Fall 1979).

26. D. R. Oden and G. D. Seybold, "DRAFT - A Computer Code for the Calculation of Fission Product Activity Ratios," Battelle Pacific Northwest Laboratory report BNWL-1607 (June 1971).

27. G. L. Hanna, "Gamma-Ray Measurement of Spent Hifar Fuel Elements for Safeguards Verification, Part I: Experimental Evaluation of Method, and Part II: Theoretical Evaluation of Method," Australian Safeguards Office reports A50/R2 and A50/R3 (July 1978).

28. C. R. Hatcher, "Errors In Spent Fuel Cooling Time Determination Due to Constant Power Approximation of Irradiation History," International Atomic Energy Agency internal memorandum, October 1979.

29. J. Valovic, V. Petenyi, S. B. Rana, D. Mikusova, and J. Kmosena, "The Application of Gamma and Isotopic Correlation Techniques for Safeguards Identification and Verification Purposes," International Atomic Energy Agency research contract 1443, Bohunice Nuclear Power Plant, Bohunice, Czechoslovakia (1975).

30. T. N. Dragnev, "Experimental Techniques for Measuring Burnup Nondestructive Techniques: Gamma Spectrometry," Interregional Review Course on Reactor Burnup Physics, Mol, Belgium, October 1974, International Atomic Energy Agency report IAEA/STR-48.

31. D. M. Lee, J. R. Phillips, S. T. Hsue, K. Kaieda, E. G. Medina, and C. R. Hatcher, "A New Approach to the Examination of LWR Fuel Assemblies Using Simple Gas Chamber Techniques," Los Alamos Scientific Laboratory report LA-7655-MS (March 1979).

32. Phillip M. Rinard, "Gamma Doses From Irradiated Assemblies Under Water," Los Alamos Scientific Laboratory report LA-7914-MS (July 1979).

33. N. R. Draper and H. Smith, Applied Regression Analysis (John Wiley and Sons, Inc., New York, 1966) p. 26.

34. P. I. Fedotov, Khlopin Radium Institute, private communication, October 1979.

35. R. A. Wolters, General Electric Co., private communication, September 1978.

36. G. R. Parkos and G. F. Valby, "Gamma Scan Measurements at Zion Station Unit 2 Following Cycle I," Electric Power Research Institute report EPRI NP-509 (October 1977).

37. M. B. Cutrone and G. F. Valby, "Gamma Scan Measurements at Quad Cities Nuclear Power Station Unit 1 Following Cycle 2," Electric Power Research Institute report EPRI NP-214 (July 1976).

38. P. Barbera, G. Bidoglio, M. Bresesti, R. Chevalier, et al, "Post-Irradiation Examination of Fuel Discharged from the TRINO Vercellese Reactor after the 2nd Irradiation Cycle," Commission of European Communities report EUR 5605-e (1976).

39. D. E. Christensen, "Collection and Analysis of Measured Fission Product Data," U.S. Arms Control and Disarmament report (March 1979).

40. C. M. Lederer and V. S. Shirley, Eds., Table of Isotopes - Seventh Edition (John Wiley and Sons, Inc., New York, 1978).

41. Nucl. Data Sheets 15, 203 (1975).

42. Nucl. Data Sheets 13, 337 (1974).

43. T. R. England, "CINDER - A One-Point Depletion and Fission Product Program," Westinghouse Electric Corporation report WAPD-TM-334 (1962, Rev. 1964).

44. T. R. England and W. B. Wilson, Los Alamos Scientific Laboratory, private communication, May 1979.

45. M. Conte, M. Mouchnino, and F. K. Schmitz, "Postirradiation Observations of Mixed Oxides with Initial Addition of Fission Product Elements," Nucl. Technol. 16, (October 1972).

46. J. R. Phillips, J. R. Netuschil, J. N. Quintana, and G. R. Waterbury, "Axial Distribution of ^{95}Nb and ^{95}Zr Isotopes in Irradiated UO_2-PuO_2 Fuel Pins," J. Inorg. Nucl. Chem. 37, 1337-1340 (1975).

47. J. R. Phillips, "New Techniques in Precision Gamma Scanning: Application to Fast-Breeder Reactor Fuel Pins," Los Alamos Scientific Laboratory report LA-5260-T (1973).

48. J. D. Chen, D. G. Boase, and R. B. Lypka, "Nondestructive Determination of Burnup by Gamma Scanning: An Assessment of $^{144}Ce/Pr$ as a Fission Monitor in CANDU Fuels," Atomic Energy Commission Limited report AECL-5236 (January 1976).

49. R. S. Forsyth and W. H. Blackadder, "Use of the Fission Product Ru-106 Gamma Activity as a Method for Estimating the Relative Number of Fission Events in ^{235}U and ^{239}Pu in Low Enriched Fuel Elements," in Safeguards Techniques, Symp. Proc., Karlsruhe, July 6-10, 1970 (International Atomic Energy Agency, Vienna, 1970) IAEA-SM-133/4, Vol. I, pp. 521-532.

50. J. A. L. Robertson, Irradiation Effects in Nuclear Fuels (Gordon and Breach, New York, 1969).

51. J. R. Phillips, G. R. Waterbury, and N. E. Vanderborgh, "Distribution of ^{134}Cs and ^{137}Cs in the Axial UO_2 Blankets of Irradiated $(U,Pu)O_2$ Fuel Pins," J. Inorg. Nucl. Chem. 36, 17-23 (1974).

52. D. Cubicciotti, J. S. Sanecki, R. V. Strain, S. Greenberg, L. A. Neimark, and C. E. Johnson, "The Nature of Fission-Product Deposits Inside LWR Fuel Rods," Proceedings of ANS Topical Meeting on Water Reactor Fuel Performance, St. Charles, Ill., May 9-11, 1979, pp. 282-294.

53. N. Fuhrman, V. Pasupathi, L. V. Consetti, "PCI Observation in a Combustion Engineering PWR, "Proceedings of ANS Topical Meeting on Water Reactor Fuel Performance, St. Charles, Ill., May 9-11, 1979, pp. 262-272.

54. D. West and A. C. Sherwood, "Neutron Yields from (α,n) Reactions in the Light Elements," (Harwell Conference, Fall 1978).

55. J. K. Bair and J. Gomez del Campo, "Neutron Yields from α-Particle Bombardment," submitted for publication in Nucl. Sci. Eng. (1979).

56. F. Manero and V. A. Konshin, "Status of the Energy-Dependent $\bar{\nu}$-Values for the Heavy Isotopes ($Z > 90$) from Thermal to 15 MeV and of the $\bar{\nu}$-Values for Spontaneous Fission," At. Energy Rev. 11, No. 4, 634 (1972).

57. H. Liskien and A. Paulsen, "Neutron Yields of Light Elements Under α-Bombardment," Atomkernennergie, 30, 59-61, (1977) Lfg. 1.

58. T. R. England, W. B. Wilson, and M. G. Stamatelatos, "Fission Product Data for Thermal Reactors, Part 2: Users' Manual for EPRI-CINDER Code and Data," Electric Power Research Institute report EPRI NP-356 (December 1976).

59. D. F. Morrison, Multivariate Statistical Methods (McGraw-Hill, New York, 1967).

☆ U.S. Government Printing Office: 1980 — 677 — 115/79